Title
Extinction Models for Cancer Stem Cell Therapy

Authors
Sehl, Mary
Zhou, Hua
Sinsheimer, Janet
et al.

Publication Date
2009-05-08

Peer reviewed

Extinction Models for Cancer Stem Cell Therapy

Mary Sehl[†], Hua Zhou[‡], Janet S. Sinsheimer[†,‡,§], and Kenneth L. Lange[†,‡,¶]

May 8, 2009

[†]*Department of Biomathematics,* [‡]*Department of Human Genetics, David Geffen School of Medicine,* [§]*Department of Biostatistics, School of Public Health,* [¶]*Department of Statistics, University of California, Los Angeles, CA 90095, USA*

Abstract

Stem cells are now viewed as initiating and sustaining many cancers. This suggests that cancer can be cured by driving cancer stem cells to extinction. The problem with this strategy is that ordinary stem cells are apt to be killed in the process. This paper sets bounds on the killing differential that must exist for the survival of an adequate number of normal stem cells. Our main tools are birth-death Markov chains in continuous time. In this framework, we investigate the extinction times of cancer stem cells and normal stem cells. Application of extreme value theory from mathematical statistics yields an accurate asymptotic distribution and corresponding moments for both extinction times. We compare these distributions for the two cell populations as a function of the killing rates. Perhaps a more telling comparison involves the number of normal stem cells N_H at the extinction time of the cancer stem cells. Conditioning on the asymptotic time to extinction of the cancer stem cells allows us to calculate the asymptotic mean and variance of N_H. The full distribution of N_H can be retrieved by the finite Fourier transform and, in some parameter regimes, by an eigenfunction expansion. Finally, we discuss the impact of quiescence (the resting state) on stem cell dynamics. Quiescence can act as a sanctuary for cancer stem cells and imperils the proposed therapy. We approach the complication of quiescence via multitype branching process models and stochastic simulation. Improvements to the τ-leaping method of stochastic simulation make it a versatile tool in this context. We conclude that the proposed therapy must target quiescent cancer stem cells as well as actively dividing cancer stem cells. The current cancer models demonstrate the virtue of attacking the same quantitative questions from a variety of modeling, mathematical, and computational perspectives.

Key words. birth-death process, cancer stem cells, extinction probability, finite Fourier transform, stochastic simulation

AMS subject classifications. 60J80, 60J85, 92B05

1 Introduction

Cancer stem cells represent a novel target of therapy that may revolutionize the treatment of cancer. Mathematical models sharpen our understanding of how cancer stem cell populations evolve and suggest optimal strategies to attack them. Because they undergo repeated divisions, stem cells accumulate mutations over time. Cells derived from stem cells start down differentiation pathways that involve a limited number of cell divisions. Once they reach the end of their pathways, diffentiated cells no longer accumulate the mutations caused by faulty DNA replication during cell division. Thus, many oncologists contend that only stem cells can drive cancer [48, 50, 59]. Because normal stem cells are vital for the maintenance and repair of tissues, safe eradication of cancer stem cells requires selectively targeting cancer stem cells while sparing normal stem cells. In the current paper we explore in depth this hypothetical strategy and discuss its implications for the design of the next generation of cancer therapeutics.

Our point of departure is the stochastic theory of linear birth-death processes. This is well trod ground mathematically [14, 25, 23, 33, 34, 36, 39], but the current problems raise novel issues not encountered in the standard treatments. For instance, how can one approximate the distribution of the extinction time for either population of stem cells? This brings in extreme-value theory from statistics, eigenfunction expansions, and the finite Fourier transform. We particularly fixate on three related questions: a) What is the killing differential that makes our hypothetical therapy viable? b) What is the distribution of the number of normal stem cells at the random time of extinction of the cancer stem cells? c) What implications does the phenomenon of quiescence have for the proposed therapy? To answer questions a) and b), we condition one birth-death process on the random extinction time of the other birth-death process. To answer question c), we turn to multi-type

branching processes, with stem cells of either kind divided into active and quiescent types. Because some of our answers are approximate, it helps to look at the same problem from multiple perspectives. This leads us to introduce the subject of stochastic simulation by τ-leaping [53]. Except for numerically unstable eigenfunction expansions, the different techniques discussed here reinforce one another and increase our confidence in the basic model.

Before presenting an overview of the rest of the paper, let us comment on the relevance of stochastic models in general and birth-death processes in particular. In a nutshell, stochastic models are ideal for studying stem cell dynamics because stem cell population sizes are small relative to total cell numbers and key events of interest are probabilistic in nature. Stem cells occupy well defined niches in the body, and it is not too hard to imagine the stem cell clans behaving independently, at least in the short run. Thus, linear birth-death processes appear to offer a good vehicle for modeling [14, 25, 23, 33, 34, 36, 39].

In the next two sections, we provide a brief overview of stem cell biology and background information on birth-death processes. In Section 4 we rederive the distribution of the extinction time for a subcritical birth-death process starting with a single cell. This classical result is inadequate for our purposes because we typically start with many cells and must track all clans issuing from them. Using extreme-value theory, we find an accurate asymptotic distribution for the time at which all clans go extinct. This result allows us to compare probability densities for the extinction times of two coexisting populations of stem cells: normal stem cells and cancer stem cells, dying at different rates under therapy. Convergence in distribution does not imply convergence of moments, so we verify in Section 4.2 convergence of the mean and variance of the extinction times to the mean and variance of the asymptotic distribution.

In Sections 4.3 and 4.4, we study the number of normal stem cells N_H remain-

ing at the random time all cancer stem cells go extinct. We derive the mean and variance for N_H by conditioning on the extinction time of cancer stem cells. These quantities are heavily dependent on the selectivity of a therapy. We also compute the full distribution of N_H using eigenvalue expansions and the finite Fourier transform. In Sections 4.5 and 4.6 we discuss the quiescent (resting) state of the stem cell, and its impact on cancer stem cell dynamics under therapies that selectively eliminate actively dividing cells. Quiescence requires new models and a different set of numerical tools. We particularly focus on simulation and τ-leaping in Section 5. Our discussion summarizes all findings and comments on the role of mathematical modeling in cancer therapy.

2 Biological Background

Let us begin by describing some biological features of stem cells that fit within the framework of birth-death processes. Two of the principal distinguishing features of stem cells are *self-renewal* and *potency* [42]. Self-renewal capacity is defined as the ability of a cell to indefinitely reproduce copies of itself at the same level of differentiation. In asymmetric cell division, a stem cell produces an identical daughter cell and a second more differentiated daughter cell. A stem cell can also divide symmetrically, giving rise to two copies of itself. Figure 1 depicts the two modes of cell division. Potency is the capacity of a stem cell to replenish all of the highly specialized cells of a tissue. Embryonic stem cells are the least differentiated of all cells. They can be coaxed into producing cells populating any of the three embryonic germ layers. These layers in turn ultimately produce all cell types in the body.

Non-embryonic stem cells lack the *totipotent* capacity of embryonic stem cells. For instance, hematopoietic stem cells can only give rise to a closely related family of cells that circulate in the blood. Figure 2 illustrates the ability of the hematopoietic

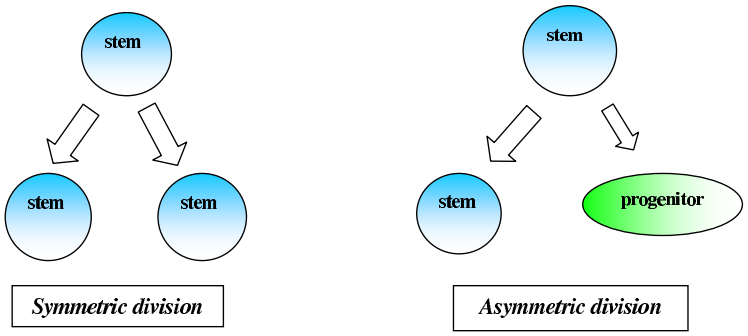

Figure 1: Self-renewal capacity of stem cells.

stem cell to generate multipotent progenitors, which can then begin the process of differentiation, either into the myeloid lineage or the lymphoid lineage. The myeloid lineage generate cells that carry oxygen to tissues (erythrocytes), cells that help with clot formation (platelets), and cells that fight acute infection (granulocytes), while the lymphoid lineage gives rise to cells of the immune system (B and T lymphocytes). It is noteworthy that progenitor cells do have the ability to self-renew, but only for a limited time. Only stem cells have the capacity for indefinite self-renewal.

Additional important features of stem cells include slow self-renewal and quiescence; these allow stem cells to maintain a long life span [42]. Different kinds of stem cells spend varying percentages of time in an actively dividing state and a quiescent (resting) state. For example, embryonic stem cells spend about 90% of the time in an actively dividing state, whereas hematopoietic stem cells are quiescent approximately 75% of the time [9]. Stem cells can enter the state of quiescence and later re-awaken. Cellular *senescence* occurs when a cell is no longer able to divide [26]. A final important defining property of stem cells is niche-dependence [42]. Stem cell niches, distributed throughout the body, serve to regulate the total number of stem cells and whether or not stem cells maintain an undifferentiated state.

Stem cells have been shown to play a role in the pathogenesis and progression

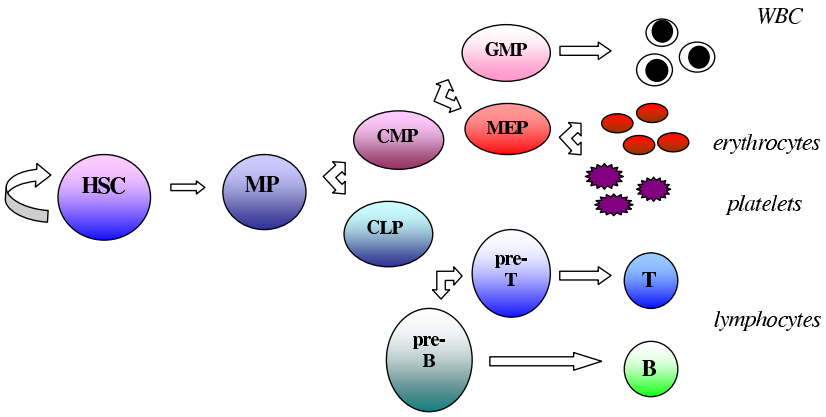

HSC = hematopoietic stem cell, MP = multipotent progenitor, CMP = common myeloid progenitor, CLP = common lymphoid progenitor, GMP = granulocyte-macrophage precursor, MEP = megakaryocyte-erythrocyte precursor, WBC = white blood cells. Curved arrow represents self-renewal.

Figure 2: Multipotency of hematopoietic stem cells.

of many malignancies, including acute myeloid leukemia [40], chronic myelogenous leukemia [58], breast cancer [2], acute lymphoblastic leukemia [10], glioblastoma [56], multiple myeloma [43], prostate cancer [32, 47, 61], colorectal cancer [45], squamous cell carcinoma of the head and neck [49], sarcoma [57], and melanoma [52]. Chronic myelogenous leukemia [16] provides some of the best evidence that mutation in a single stem cell can give rise cancer. Here one can follow the full cascade of tumor cell types from malignant stem cells to progenitors on to fully differentiated cells. Cancer stem cells have also been implicated in the development of resistance to therapy [4, 31, 35, 41]. Finally, the deleterious effects of extinction of a population of normal stem cells is not just a matter of conjecture. For example, deletion of the ATR gene in adult mice causes extinction of stem cells and leads to premature aging manifested by allopecia and osteoporosis [51].

Therapies that target cancer stem cells have recently been proposed. These

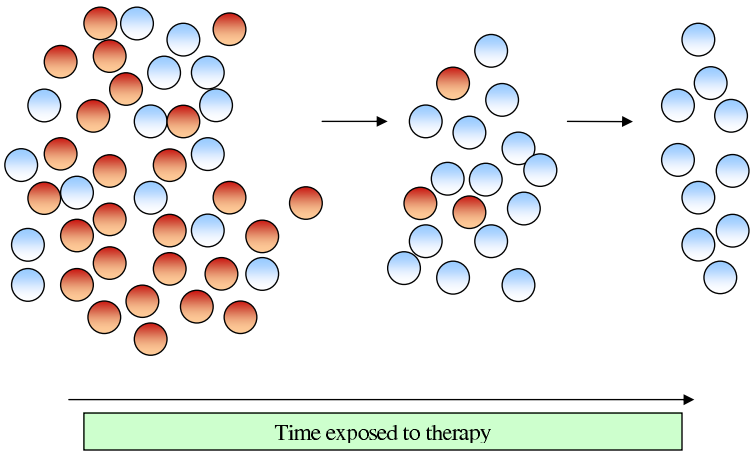

Figure 3: Selective destruction of cancer stem cells under targeted therapy.

include monoclonal antibody therapy [46], vaccine therapy [13], drugs targeting the Notch signaling pathway [55], and other targeted therapies [5, 24, 62, 63]. Several therapies are currently being proposed to selectively eliminate cancer stem cells while sparing normal stem cells. For example, a sesquiterpene lactone called parthenolide has been shown to cause induce programmed cell death in leukemic stem cells, while leaving relatively large populations of normal hematopoietic cells [24]. Figure 3 demonstrates the basic biological question we address with modeling. While exposed to a therapy targeting cancer stem cells, cancer stem cells (in red) are selectively eliminated, while the normal stem cells (in blue) are also killed, but at a slower rate. After some length of time, all cancer stem cells are eliminated while a population of surviving ordinary stem cells remains. In our opinion, the critical question is whether the number of surviving normal stem cells remains above the threhshold adequate to maintain tissue homeostasis.

3 Background on Linear Birth-Death Processes

In our simplified model of therapy, there are two populations of stem cells, normal stem cells and cancer stem cells. These coexisting populations do not interact. The cancer stem cells originate by a sequence of mutations from the normal stem cells. We take the existence of cancer stem cells as given and ignore repeated transitions to the cancer state. We model each population as a linear birth-death process X_t in continuous time t with constant birth rate β and constant death rate δ per particle. The process X_t counts the number of particles at time t. Birth-death processes have been the subject of extensive study for many decades [14, 25, 23, 33, 34, 36, 39]. For the convenience of the reader, we now summarize some basic facts.

Let us begin by heuristically deriving the mean and variance of X_t. These moments are determined by the infinitesimal mean and variance of the increment $X_{t+s} - X_t$. Over a short time interval, it is obvious that

$$\begin{aligned}
\mathbb{E}\left(X_{t+s} - X_t \mid X_t = x\right) &= \beta xs1 + \delta xs(-1) + o(s) \\
&= (\beta - \delta)xs + o(s) \\
\mathbb{V}\mathrm{ar}(X_{t+s} - X_t \mid X_t = x) &= \beta xs1^2 + \delta xs(-1)^2 + o(s) - [(\beta - \delta)xs + o(s)]^2 \\
&= (\beta + \delta)xs + o(s).
\end{aligned}$$

If we take expectations in the equation

$$\mathbb{E}\left(X_{t+s} \mid X_t\right) = X_t + (\beta - \delta)X_t s + o(s),$$

form the corresponding difference quotient, and send s to 0, then we arrive at the ordinary differential equation

$$\frac{d}{dt}\mathbb{E}\left(X_t\right) = (\beta - \delta)\,\mathbb{E}\left(X_t\right)$$

with solution

$$\mathbb{E}\left(X_t\right) = \mathbb{E}\left(X_0\right)e^{(\beta-\delta)t}. \tag{1}$$

To derive a differential equation for the variance, we reason that

$$\begin{aligned}
\mathbb{V}\text{ar}(X_{t+s}) &= \mathbb{E}\left[\mathbb{V}\text{ar}(X_{t+s} \mid X_t)\right] + \mathbb{V}\text{ar}[\mathbb{E}\left(X_{t+s} \mid X_t\right)] \\
&= \mathbb{E}\left[\mathbb{V}\text{ar}(X_{t+s} - X_t \mid X_t)\right] + \mathbb{V}\text{ar}[X_t + (\beta - \delta)X_t s + o(s)] \\
&= \mathbb{E}\left[(\beta + \delta)X_t s + o(s)\right] + [1 + (\beta - \delta)s]^2 \mathbb{V}\text{ar}(X_t) + o(s) \\
&= (\beta + \delta)\,\mathbb{E}\left(X_t\right)s + [1 + 2(\beta - \delta)s]\,\mathbb{V}\text{ar}(X_t) + o(s).
\end{aligned}$$

Once again we form the difference quotient and send s to 0. These maneuvers yield the ordinary differential equation

$$\frac{d}{dt}\mathbb{V}\text{ar}(X_t) = (\beta + \delta)\,\mathbb{E}\left(X_t\right) + 2(\beta - \delta)\,\mathbb{V}\text{ar}(X_t)$$

with solution

$$\mathbb{V}\text{ar}(X_t) = \mathbb{V}\text{ar}(X_0)e^{2(\beta-\delta)t} + \mathbb{E}\left(X_0\right)\frac{(\beta + \delta)}{(\beta - \delta)}\left[e^{2(\beta-\delta)t} - e^{(\beta-\delta)t}\right]. \tag{2}$$

For our purposes, X_0 is a constant n, so $\mathbb{E}\left(X_0\right) = n$ and $\mathbb{V}\text{ar}(X_0) = 0$.

Extinction is certain in a linear birth-death process in the subcritical case $\beta < \delta$. Fortunately, it is possible to calculate exactly the distribution function $F(t)$ of the extinction time starting with a single particle at time 0. The standard argument hinges on the time until the first event, either a birth or death. This waiting time is exponentially distributed with intensity $\eta = \beta + \delta$. At the end of the waiting time, the initial particle dies with probability $p_0 = \delta/\eta$ or gives birth with probability $p_2 = \beta/\eta$. In the latter case, the clans issuing from the mother and daughter particles behave independently and, in a stochastic sense, identically. These considerations imply that

$$F(t + s) = (1 - \eta s)F(t) + \eta s p_0 1 + \eta s p_2 F(t)^2 + o(s)$$

Forming the difference quotient and sending s to 0 now produce the ordinary differential equation

$$\frac{d}{dt}F(t) = -(\beta + \delta)F(t) + \delta + \beta F(t)^2$$

of Ricatti type with initial condition $F(0) = 0$. The solution

$$F(t) \;=\; \frac{\delta - \delta e^{(\beta-\delta)t}}{\delta - \beta e^{(\beta-\delta)t}}. \tag{3}$$

can be easily checked. Note that $F(t)$ is the value of the well-known probability generating function

$$E(s^{X_t}) \;=\; 1 + \frac{1}{\left(\frac{1}{s-1} - \frac{\beta}{\delta-\beta}\right) e^{(\delta-\beta)t} + \frac{\beta}{\delta-\beta}} \tag{4}$$

at $s = 0$ [39].

4 Stem Cell Extinction Times under Therapy

The major theme of this paper is the comparison of the times until extinction of the two stem cell populations. We now apply and refine the elementary results of the last section.

4.1 Extinction Times with Multiple Clans

Suppose we start with n stem cells at time 0. If T_i denotes the time of extinction of the clan emanating from stem cell i, then we are interested in the time $M_n = \max_i T_i$ at which all n clans go extinct. Assuming that each clan behaves independently as a linear birth-death process with parameters β and δ, the distribution of M_n is

$$\Pr(M_n \leq t) \;=\; F(t)^n,$$

where $F(t)$ is given by equation (3). Fortunately, we can apply the asymptotic theory of extreme order statistics [15] to understand the distribution of M_n. The standard case of the theory says that there are two sequences of constants a_n and b_n such that

$$\lim_{n\to\infty} \Pr\left(\frac{M_n - a_n}{b_n} \leq t\right) \;=\; \lim_{n\to\infty} \Pr(M_n \leq a_n + b_n t) \;=\; e^{-e^{-t}} \tag{5}$$

for all t. The extreme value (Gumbel) distribution $\exp(-e^{-t})$ has mean γ and variance $\pi^2/6$, where $\gamma \approx 0.57722$ is the Euler-Mascheroni constant. The moment generating function of the extreme value distribution can be written for argument θ as

$$\int_{-\infty}^{\infty} e^{\theta x} e^{-x} e^{-e^{-x}} dx \;=\; \Gamma(1-\theta) \tag{6}$$

in terms of Euler's gamma function. It is plausible that

$$\mathbb{E}\,(M_n) \;\approx\; a_n + \gamma b_n, \quad \mathbb{V}\mathrm{ar}(M_n) \;\approx\; \frac{b_n^2 \pi^2}{6},$$

and we will prove this later.

The key to finding the sequences a_n and b_n is to identify a function $R(t)$ such that

$$\lim_{t \to \infty} \frac{1 - F[t + xR(t)]}{1 - F(t)} \;=\; e^{-x} \tag{7}$$

for all x. (See Theorem 14 of [15].) Once we have $R(t)$ in hand, we determine a_n and b_n via the equations $1 - F(a_n) = \frac{1}{n}$ and $b_n = R(a_n)$. In the current situation, $R(t)$ is the constant $(\delta - \beta)^{-1}$. The equation

$$\frac{1}{n} \;=\; 1 - F(a_n) \;=\; 1 - \frac{\delta - \delta e^{(\beta-\delta)a_n}}{\delta - \beta e^{(\beta-\delta)a_n}} \;=\; \frac{\delta - \beta}{\delta e^{(\delta-\beta)a_n} - \beta}$$

entails

$$\frac{n(\delta - \beta) + \beta}{\delta} \;=\; e^{(\delta-\beta)a_n},$$

which in turn implies

$$a_n \;=\; \frac{1}{\delta - \beta}\Big[\ln n + \ln\Big(\frac{\delta - \beta + \frac{\beta}{n}}{\delta}\Big)\Big]. \tag{8}$$

It follows that $\mathbb{E}\,(M_n)$ grows at the slow rate $\ln n$ and $\mathbb{V}\mathrm{ar}(M_n)$ tends to the constant $\pi^2/[6(\delta - \beta)^2]$.

These conclusions are all predicated on satisfaction of condition (7). In view of equation (3), we have

$$\begin{aligned}\lim_{t\to\infty}\frac{1-F[t+xR(t)]}{1-F(t)} &= \lim_{t\to\infty}\frac{1-\frac{\delta e^{(\delta-\beta)t+x}-\delta}{\delta e^{(\delta-\beta)t+x}-\beta}}{1-\frac{\delta e^{(\delta-\beta)t}-\delta}{\delta e^{(\delta-\beta)t}-\beta}}\\ &= \lim_{t\to\infty}\frac{\delta e^{(\delta-\beta)t}-\beta}{\delta e^{(\delta-\beta)t+x}-\beta}\\ &= e^{-x}.\end{aligned}$$

This proves condition (7) and validates all of the conclusions drawn from it.

We can also solve for the time t that renders the extinction probability $F(t)^n$ equal to a given number $p > 0$. Since

$$\lim_{n\to\infty}\frac{1-p^{\frac{1}{n}}}{\frac{1}{n}} = -\frac{d}{dx}\left(p^x\right)|_{x=0} = -\ln p,$$

we have

$$\ln\left[n(1-p^{\frac{1}{n}})\right] \approx \ln(-\ln p).$$

In view of the identity (3), the solution of the equation $p = F(t)^n$ therefore satisfies

$$\begin{aligned}t &= -\frac{1}{\delta-\beta}\ln\left(\frac{\delta-\delta p^{1/n}}{\delta-\beta p^{1/n}}\right)\\ &= \frac{1}{\delta-\beta}\left\{\ln\left(\delta-\beta p^{\frac{1}{n}}\right)-\ln\delta+\ln n-\ln\left[n(1-p^{\frac{1}{n}})\right]\right\} \qquad (9)\\ &\approx a_n-\frac{1}{\delta-\beta}\ln(-\ln p).\end{aligned}$$

This is precisely the approximation the extreme value theory entails.

As an illustration of our results, consider an advanced form of leukemia. We now have separate birth rates, death rates, and initial numbers of stem cells, which we subscript by the index H for healthy and C for cancerous, corresponding to the normal hematopoietic stem cell (HSC) and cancer stem cell (CSC) populations. Total initial hematopoietic stem cell population size $(22,000)$ is based on numbers

extrapolated from murine and feline data [1]. Because recent evidence suggests that HSCs divide approximately once every 42 weeks [1], we chose our birth rates $\beta_H = \beta_C = 0.02$ week^{-1}. Suppose for the sake of argument, we start with $n_H = 4,400$ and $n_C = 17,600$ and take $\delta_H = 0.08$ week^{-1}, and $\delta_C = 0.59$ week^{-1}. Our asymptotic results allow us to examine the probability densities of the extinction times of both CSCs and HSCs. The top panel of Figure 4 shows that the asymptotic probability density of the extinction time of CSCs has a narrow spike around 18 weeks, whereas that of HSCs has a narrow spike around 139 weeks. We observe good agreement between results obtained using the Gumbel approximation and exact results obtained by differentiating the distribution function. There is very little overlap between the two extinction-time densities. This suggests that for the given parameter values, most likely the CSCs would be eradicated long before the HSCs become extinct. The appearance of these probability density curves confirms a wide therapeutic window of opportunity. However, when we take the death rates $\delta_H = 0.31$ week^{-1}, and $\delta_C = 0.59$ week^{-1}, the densities displayed in the bottom panel of Figure 4) dangerously overlap.

The weak $\ln n$ dependence of the sequence a_n on n suggests the possibility of safely eradicating CSCs even when they sharply outnumber HSCs. In this regard, it is helpful to define the selectivity σ of a therapy as the ratio

$$\sigma = \frac{\delta_C - \beta_C}{\delta_H - \beta_H}$$

of the differences between death and birth rates for CSCs versus HSCs. For safe eradication one needs σ to be substantially greater than $\ln n_C / \ln n_H$.

Passing back and forth between the formulas (3) and (10) allows us to plot the extinction probability for the HSCs at the time when the extinction probability for the CSCs reaches a predetermined level p. The survival probability of the HSC population increases fairly quickly as the difference between δ_H and δ_C grows. For example, take $\delta_H = 0.08$ week^{-1} and $\beta_C = \beta_H = 0.02$ week^{-1}. To be 80% certain

that at least one ordinary stem cell remains when we are 99.9% certain no CSC remains, δ_C must be 0.15 week^{-1} or larger, corresponding to $s \geq 2.2$.

4.2 Convergence of Extinction Time Moments

The convergence in distribution displayed in equation (5) does not necessarily entail convergence of moments. We address this delicate question first for means. Our point of departure is the right-tail integral

$$\mathbb{E}\,(M_n) \;=\; \int_0^\infty \Pr(M_n > t)\,dt \;=\; \int_0^\infty \Big\{1 - \Big[\frac{\delta - \delta e^{(\beta-\delta)t}}{\delta - \beta e^{(\beta-\delta)t}}\Big]^n\Big\}dt$$

for the mean of M_n. To gain insight into how this integral depends on n, we make the change of variables

$$s \;=\; \frac{\delta - \delta e^{(\beta-\delta)t}}{\delta - \beta e^{(\beta-\delta)t}}, \qquad t \;=\; -\frac{1}{(\delta-\beta)}\ln\frac{\delta-\delta s}{\delta-\beta s}. \tag{10}$$

The change of variables implies the change in differentials

$$dt \;=\; \Big[\frac{1}{(\delta-\beta)(1-s)} - \frac{\beta}{(\delta-\beta)(\delta-\beta s)}\Big]ds \tag{11}$$

and the range of integration $(0,1)$ for s. Since

$$\frac{1-s^n}{1-s} \;=\; (1 + s + \cdots + s^{n-1}),$$

it follows that

$$\begin{aligned}
\mathbb{E}\,(M_n) &= \int_0^1 (1-s^n)\Big[\frac{1}{(\delta-\beta)(1-s)} - \frac{\beta}{(\delta-\beta)(\delta-\beta s)}\Big]ds \\
&= \frac{1}{\delta-\beta}\Big[1 + \frac{1}{2} + \cdots + \frac{1}{n}\Big] - \int_0^1 \frac{(1-s^n)\beta}{(\delta-\beta)(\delta-\beta s)}ds \qquad (12)\\
&= \frac{1}{\delta-\beta}[\ln n + \gamma] + \frac{1}{\delta-\beta}\ln\Big(\frac{\delta-\beta}{\delta}\Big) + O\Big(\frac{1}{n}\Big),
\end{aligned}$$

where γ enters the picture through the well-known expansion

$$H_n \;=\; \ln n + \gamma + \frac{1}{2n} + O\Big(\frac{1}{n^2}\Big)$$

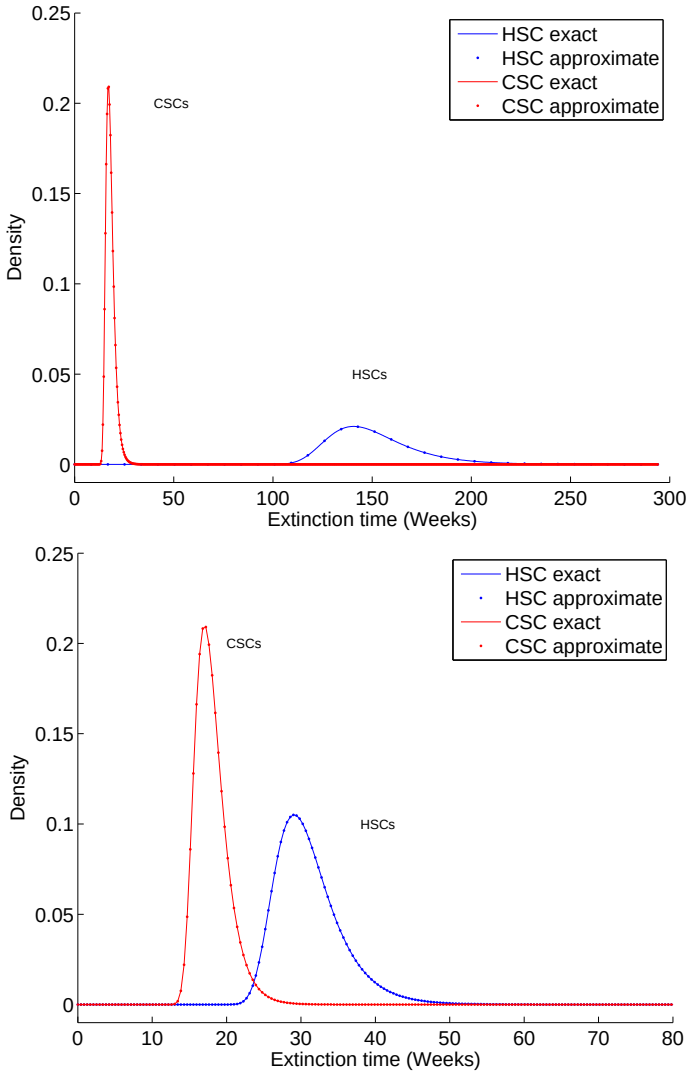

Figure 4: Extinction time densities for CSCs and HSCs. Top: $\delta_C = 0.59$ week^{-1}, $\delta_H = 0.08$ week^{-1}. Bottom: $\delta_C = 0.59$ week^{-1}, $\delta_C = 0.31$ week^{-1}.

of the harmonic sum $H_n = 1 + \frac{1}{2} + \cdots + \frac{1}{n}$ [22], and

$$\frac{\beta}{\delta - \beta} \int_0^1 \frac{s^n}{\delta - \beta s} ds \quad = \quad O\Big(\frac{1}{n}\Big)$$

by virtue of the boundedness of $1/(\delta - \beta s)$ on $[0, 1]$. Our formula for $\mathbb{E}\,(M_n)$ confirms the limit

$$\lim_{n \to \infty} \mathbb{E}\,\Big(\frac{M_n - a_n}{b_n}\Big) \quad = \quad \gamma.$$

We now validate a similar limit for the variance of the extinction times. Expressing the second moment as an integral of the right-tail probability and taking into account equations (10) and (11) produce

$$\begin{aligned} \mathbb{E}\,(M_n^2) &= 2 \int_0^\infty t \Pr(M_n > t)\, dt \\ &= -\frac{2}{(\delta - \beta)^2} \int_0^1 \ln\left(\frac{1 - s}{1 - \frac{\beta}{\delta} s}\right) (1 - s^n) \Big[\frac{1}{(1 - s)} - \frac{\beta}{(\delta - \beta s)}\Big] ds. \end{aligned} \tag{13}$$

We will attack the integral (13) in piecemeal fashion. For instance,

$$\begin{aligned} \int_0^1 (1 - s^n) \frac{\ln(1 - s)}{1 - s} ds &= \int_0^1 \ln(1 - s) \sum_{k=0}^{n-1} s^k ds \\ &= -\int_0^1 \sum_{j=1}^{\infty} \frac{s^j}{j} \sum_{k=0}^{n-1} s^k ds \\ &= -\sum_{j=1}^{\infty} \sum_{k=0}^{n-1} \frac{1}{j(j + k + 1)} \\ &= -\sum_{j=1}^{\infty} \sum_{k=0}^{n-1} \Big(\frac{1}{j} - \frac{1}{j + k + 1}\Big) \frac{1}{k + 1} \\ &= -\sum_{k=0}^{n-1} \frac{1}{k + 1} \Big(1 + \frac{1}{2} + \cdots + \frac{1}{k + 1}\Big) \\ &= -\sum_{k=1}^{n} \frac{H_k}{k}. \end{aligned}$$

Fortunately, the two further helpful identities

$$\sum_{k=1}^{n} \frac{H_k}{k} \;=\; \frac{1}{2}\Big(\sum_{k=1}^{n} \frac{1}{k^2} + H_n^2\Big), \qquad \sum_{k=1}^{\infty} \frac{1}{k^2} \;=\; \frac{\pi^2}{6}$$

are true [22]. It follows that

$$\int_0^1 (1-s^n)\frac{\ln(1-s)}{1-s}ds \;=\; -\frac{1}{2}\Big[\frac{\pi^2}{6} + (\ln n + \gamma)^2\Big] + O\Big(\frac{\ln n}{n}\Big).$$

Another piece of the integral (13) is amenable to the fundamental theorem of calculus; namely,

$$\beta\int_0^1 \frac{\ln(1-\frac{\beta}{\delta}s)}{\delta-\beta s}ds \;=\; -\frac{1}{2}\Big[\ln\Big(1-\frac{\beta}{\delta}s\Big)\Big]^2\Big|_0^1 \;=\; -\frac{1}{2}\Big[\ln\Big(1-\frac{\beta}{\delta}\Big)\Big]^2.$$

The integral

$$\int_0^1 \beta s^n \frac{\ln\Big(1-\frac{\beta}{\delta}s\Big)}{\delta-\beta s}ds \;=\; O\Big(\frac{1}{n}\Big)$$

because $(\delta-\beta s)^{-1}$ and $\ln(\delta-\beta s)$ are bounded on $[0,1]$. Likewise,

$$\int_0^1 \beta s^n \frac{\ln(1-s)}{\delta-\beta s}ds \;=\; O\Big(\frac{\ln n}{n}\Big)$$

because

$$\begin{aligned}
\int_0^1 s^n \ln(1-s)ds &= -\int_0^1 \sum_{j=1}^{\infty} \frac{1}{j} s^{n+j} ds \\
&= -\sum_{j=1}^{\infty} \frac{1}{j(n+j+1)} \\
&= O\Big(\frac{\ln n}{n}\Big).
\end{aligned}$$

Two other parts of the integral partially cancel. The first part amounts to

$$\begin{aligned}
-\int_0^1 \ln\Big(1-\frac{\beta}{\delta}s\Big)\frac{1-s^n}{1-s}ds &= \int_0^1 \sum_{j=1}^{\infty} \Big(\frac{\beta}{\delta}\Big)^j \frac{s^j}{j} \sum_{k=0}^{n-1} s^k ds \\
&= \sum_{j=1}^{\infty} \Big(\frac{\beta}{\delta}\Big)^j \frac{1}{j} \sum_{k=0}^{n-1} \frac{1}{j+k+1} \\
&= \sum_{j=1}^{\infty} \Big(\frac{\beta}{\delta}\Big)^j \frac{1}{j}(H_{n+j} - H_j).
\end{aligned}$$

The second part is

$$\begin{aligned} -\int_0^1 \beta \ln(1-s)\frac{1}{\delta-\beta s}ds &= \frac{\beta}{\delta}\int_0^1 \sum_{k=1}^{\infty}\frac{s^k}{k}\sum_{j=0}^{\infty}\Big(\frac{\beta}{\delta}\Big)^j s^j ds \\ &= \sum_{j=1}^{\infty}\Big(\frac{\beta}{\delta}\Big)^j \sum_{k=1}^{\infty}\frac{1}{k(j+k)} \\ &= \sum_{j=1}^{\infty}\Big(\frac{\beta}{\delta}\Big)^j \frac{1}{j}\sum_{k=1}^{\infty}\Big(\frac{1}{k}-\frac{1}{j+k}\Big) \\ &= \sum_{j=1}^{\infty}\Big(\frac{\beta}{\delta}\Big)^j \frac{1}{j}H_j. \end{aligned}$$

The sum of these two parts is

$$\begin{aligned} \sum_{j=1}^{\infty}\Big(\frac{\beta}{\delta}\Big)^j \frac{1}{j}H_{n+j} &= \sum_{j=1}^{\infty}\Big(\frac{\beta}{\delta}\Big)^j \frac{1}{j}\Big[\ln(n+j)+\gamma+O\Big(\frac{1}{n}\Big)\Big] \\ &= \sum_{j=1}^{\infty}\Big(\frac{\beta}{\delta}\Big)^j \frac{1}{j}\ln\Big(\frac{n+j}{n}\Big)+\sum_{j=1}^{\infty}\Big(\frac{\beta}{\delta}\Big)^j \frac{1}{j}(\ln n+\gamma)+O\Big(\frac{1}{n}\Big) \\ &= \sum_{j=1}^{\infty}\Big(\frac{\beta}{\delta}\Big)^j \frac{1}{j}\ln\Big(1+\frac{j}{n}\Big)-(\ln n+\gamma)\ln\Big(1-\frac{\beta}{\delta}\Big)+O\Big(\frac{1}{n}\Big) \end{aligned}$$

Because $\ln(1+x)\le x$ for $x>0$, it follows that

$$\sum_{j=1}^{\infty}\Big(\frac{\beta}{\delta}\Big)^j \frac{1}{j}\ln\Big(1+\frac{j}{n}\Big) \le \frac{1}{n}\sum_{j=1}^{\infty}\Big(\frac{\beta}{\delta}\Big)^j = O\Big(\frac{1}{n}\Big).$$

Putting together the various parts of the integral (13) and multiplying by $-\frac{2}{(\delta-\beta)^2}$ give

$$\mathbb{E}\,(M_n^2) = \frac{1}{(\delta-\beta)^2}\Big\{\frac{\pi^2}{6}+\Big[\ln n+\gamma+\ln\Big(\frac{\delta-\beta}{\delta}\Big)\Big]^2\Big\}+O\Big(\frac{\ln n}{n}\Big).$$

In view of the asymptotic expression (12) for the mean, we have

$$\mathbb{V}\mathrm{ar}\,\Big(\frac{M_n-a_n}{b_n}\Big) = \frac{\pi^2}{6}+O\Big(\frac{\ln n}{n}\Big),$$

which implies the convergence of the variance of $b_n^{-1}(M_n-a_n)$ to the variance of the Gumbel distribution.

4.3 How Many HSCs Remain When CSCs Go Extinct?

The single most important measure of success in therapy is the count of HSCs when the cancer stem cells go extinct. This is a difficult issue to attack mathematically because one must take a snapshot of the HSC population at a random stopping time. Let N_H be the number of HSCs at the random time D_C when the cancer stem cells are eradicated. This notation is consistent with the convention in this section of subscripting all quantities by either H and C to indicate the HSC population and the CSC population, respectively. To make progress, we make the simplifying assumption that the random variable

$$\frac{M_{n_C} - a_{n_C}}{b_{n_C}}$$

conforms exactly to the extreme value distribution. To recover the mean and variance of N_H, we condition on D_C in the formulas

$$\begin{aligned} \mathbb{E}(N_H) &= \mathbb{E}[\mathbb{E}(N_H \mid D_C)] && (14) \\ \mathbb{V}\text{ar}(N_H) &= \mathbb{E}[\mathbb{V}\text{ar}(N_H \mid D_C)] + \mathbb{V}\text{ar}[\mathbb{E}(N_H \mid D_C)]. && (15) \end{aligned}$$

Consider first the mean of N_H. According to equation (1), we have

$$\mathbb{E}(N_H \mid D_C) = n_H e^{(\beta_H - \delta_H)D_C}.$$

Thus, equation (14) shows that evaluation of $\mathbb{E}(N_H)$ boils down to evaluation of the moment generating function of D_C. In view of equation (6), D_C has moment generating function

$$\mathbb{E}(e^{\theta M_{n_C}}) = e^{a_{n_C}\theta}\Gamma\Big(1 - \theta b_{n_C}\Big). \quad (16)$$

A brief calculation now gives

$$\mathbb{E}(N_H) = n_H\Gamma\left(1 + \frac{\delta_H - \beta_H}{\delta_C - \beta_C}\right)\left[\frac{n_C(\delta_C - \beta_C) + \beta_C}{\delta_C}\right]^{-\frac{\delta_H - \beta_H}{\delta_C - \beta_C}}.$$

To calculate the variance of N_H from the decomposition (15), we note that equation (2) implies

$$\mathbb{V}\mathrm{ar}(N_H \mid D_C) \;=\; n_H \frac{(\beta_H+\delta_H)}{(\beta_H-\delta_H)}\left[e^{2(\beta_H-\delta_H)D_C} - e^{(\beta_H-\delta_H)D_C}\right].$$

Invoking the generating function (16) therefore yields

$$\begin{aligned} & \mathbb{E}\left[\mathbb{V}\mathrm{ar}(N_H \mid D_C)\right] \\ = \;& n_H \frac{(\beta_H+\delta_H)}{(\beta_H-\delta_H)}\Gamma\left(1+2\frac{\delta_H-\beta_H}{\delta_C-\beta_C}\right)\left[\frac{n_C(\delta_C-\beta_C)+\beta_C}{\delta_C}\right]^{-2\frac{\delta_H-\beta_H}{\delta_C-\beta_C}} \\ & - n_H \frac{(\beta_H+\delta_H)}{(\beta_H-\delta_H)}\Gamma\left(1+\frac{\delta_H-\beta_H}{\delta_C-\beta_C}\right)\left[\frac{n_C(\delta_C-\beta_C)+\beta_C}{\delta_C}\right]^{-\frac{\delta_H-\beta_H}{\delta_C-\beta_C}}. \end{aligned} \tag{17}$$

We handle the second term on the right of equation (15) by first noting that $\mathbb{E}\left[\mathbb{E}\left(N_H \mid D_C\right)\right] = \mathbb{E}\left(N_H\right)$. We combine this with

$$\begin{aligned} \mathbb{E}\left[\mathbb{E}\left(N_H \mid D_C\right)^2\right] &= n_H^2\, \mathbb{E}\left[e^{2(\beta_H-\delta_H)D_C}\right] \\ &= n_H^2 \Gamma\left(1+2\frac{\delta_H-\beta_H}{\delta_C-\beta_C}\right)\left[\frac{n_C(\delta_C-\beta_C)+\beta_C}{\delta_C}\right]^{-2\frac{\delta_H-\beta_H}{\delta_C-\beta_C}} \end{aligned}$$

to get

$$\begin{aligned} \mathbb{V}\mathrm{ar}[\mathbb{E}\left(N_H \mid D_C\right)] \;=\; & n_H^2 \Gamma\left(1+2\frac{\delta_H-\beta_H}{\delta_C-\beta_C}\right)\left[\frac{n_C(\delta_C-\beta_C)+\beta_C}{\delta_C}\right]^{-2\frac{\delta_H-\beta_H}{\delta_C-\beta_C}} \\ & - n_H^2 \Gamma\left(1+\frac{\delta_H-\beta_H}{\delta_C-\beta_C}\right)^2\left[\frac{n_C(\delta_C-\beta_C)+\beta_C}{\delta_C}\right]^{-2\frac{\delta_H-\beta_H}{\delta_C-\beta_C}}. \end{aligned} \tag{18}$$

Equations (15), (17), and (18) fully determine $\mathbb{V}\mathrm{ar}(N_H)$.

Let us define the *killing efficiency* κ of a therapy as the ratio of the death rate to birth rate of CSCs, $\kappa = \delta_C/\beta_C$. We can then formulate the mean number of HSCs present at the time when all the CSCs are eradicated as a function of the selectivity σ of a therapy and the killing efficiency, according to the formula

$$\mathbb{E}\left(N_H\right) \;\approx\; n_H \Gamma\left(1+\sigma^{-1}\right)\left[n_C(1-\kappa^{-1})+\kappa^{-1}\right]^{-\frac{1}{\sigma}}. \tag{19}$$

The variance can also be formulated as a function of κ and σ. Figure 5 plots the average $\mathbb{E}(N_H)$ as a function of σ and κ. A higher selectivity entails a higher average number of HSCs at the time of eradication of the CSCs. For example, starting with $n_H = 4,400$ and $n_C = 17,600$, with a killing efficiency $\kappa = 25$, and a selectivity $\sigma = 10$ or greater, we expect approximately 1,581 HSCs to survive. It is noteworthy that the selectivity required to ensure that, on average, $1,000$ HSCs remain at the time of CSC extinction ($\sigma = 10$) is much higher than the selectivity required to be 80% sure that at least one HSC survives ($\sigma = 2.2$). Values of the average $\mathbb{E}(N_H)$ are heavily dominated by σ. Examination of equation (19) reveals that κ is less important in determining the average $\mathbb{E}(N_H)$. In contrast, κ does play a large role in determining the average time to eradication of the CSCs. For instance with σ held constant at 10, the extinction time is approximately 4 years when $\kappa = 3$ and 18 weeks when $\kappa = 25$). The corresponding values for $\mathbb{E}(N_H)$ are 1,640 and 1,581.

4.4 Eigenfunction Expansions and Finite Fourier Transforms

Previous sections have dealt with means and variances. Finding the full distribution of the number of HSCs at the time of extinction of the CSCs requires new techniques. Here we explore two possibilities, eigenfunction expansions and Fourier analysis. Despite their elegance, eigenfunction expansions turn out to be far less reliable than approximations based on the finite Fourier transform.

The dynamics of linear birth-death processes that reach equilibrium are well encapsulated by the classical Karlin-McGregor spectral representation [33]. This formula applies to a general birth-death process with birth rate λ_n and death rate μ_n in state n, where n in this case is the number of cells of a certain type. All of these rates are positive except for $\mu_0 = 0$. If $p_{mn}(t)$ denotes the probability that the system occupies state n at time t given that it starts in state m at time 0, then the

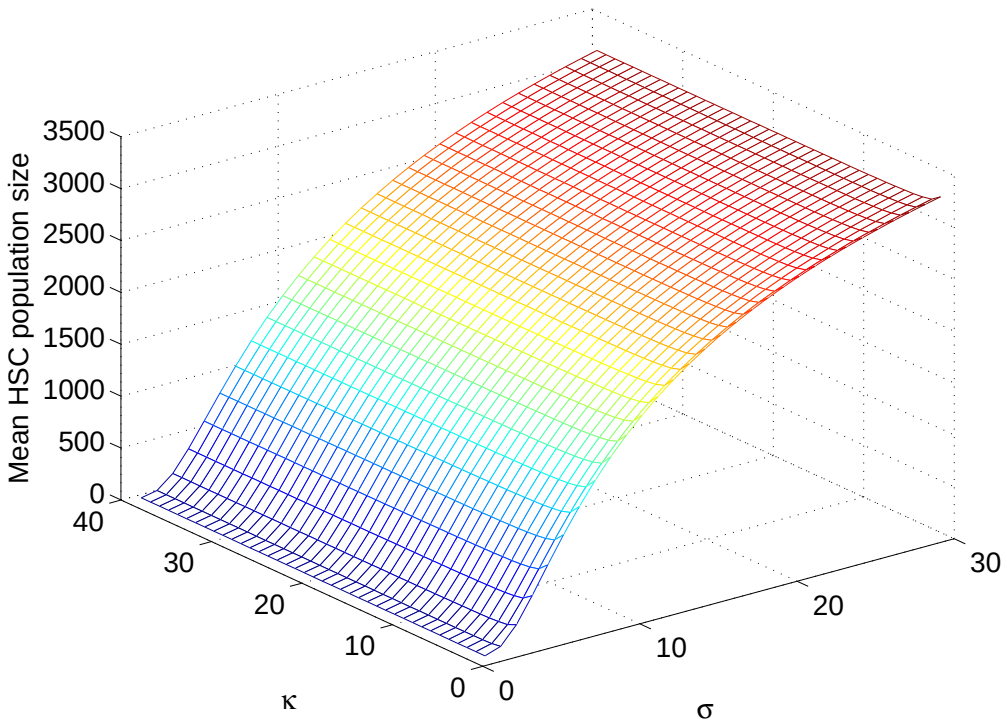

Figure 5: Dependence of $\mathbb{E}(N_H)$ on selectivity σ and killing efficiency κ of a therapy.

forward and backward equations

$$\begin{aligned}\frac{d}{dt}p_{mn}(t) &= \lambda_{n-1}p_{m,n-1}(t) - (\lambda_n + \mu_n)p_{mn}(t) + \mu_{n+1}p_{m,n+1}(t)\\ \frac{d}{dt}p_{mn}(t) &= \lambda_m p_{m+1,n}(t) - (\lambda_m + \mu_m)p_{mn}(t) + \mu_m p_{m-1,n}(t)\end{aligned}$$

govern the evolution of the system subject to the initial conditions $p_{mn}(0) = 1_{\{m=n\}}$. The Karlin-McGregor representation constitutes a diagonalization of the matrix exponential of infinite dimension solving the forward and backward equations. It is based on a finite spectral measure ω and corresponding set of orthogonal polynomials $q_n(x)$. The representation reads

$$p_{mn}(t) = \pi_n \int_0^\infty e^{-xt} q_m(x) q_n(x) d\omega(x), \tag{20}$$

where the vector π with components

$$\pi_0 = 1, \quad \pi_n = \frac{\lambda_0 \lambda_1 \cdots \lambda_{n-1}}{\mu_1 \mu_2 \cdots \mu_n}, \quad n > 0,$$

is the equilibrium distribution up to a normalizing constant. The orthogonality relations $\int_0^\infty q_m(x) q_n(x) d\omega(x) = 1_{\{m=n\}} \pi_n^{-1}$ are designed to capture the initial conditions $p_{mn}(0) = 1_{\{m=n\}}$. If we choose $q_0(x) = 1$, then the normalizing constant necessarily equals the mass that ω assigns to the point 0. The recurrence

$$-xq_n(x) = \lambda_n q_{n+1}(x) - (\lambda_n + \mu_n) q_n(x) + \mu_n q_{n-1}(x),$$

starting with $q_{-1}(x) = 0$ and $q_0(x)$ constant, ensures the validity of the forward equations. It also guarantees that $q_n(0) = q_0(0)$ for all n.

Unfortunately, the Karlin-McGregor formula (20) does not apply to our model with $\lambda_n = n\beta$ and $\mu_n = n\delta$ because $\lambda_0 = 0$. We can force compliance by introducing immigration. This corresponds to taking $\lambda_n = n\beta + \beta\lambda$, where $\beta\lambda$ is the immigration rate. In the altered model, the process reaches a nontrivial equilibrium in the

subcritical setting $\beta < \delta$. One can also show that the spectral measure follows a negative binomial distribution putting probability

$$\omega(\{(\delta-\beta)x\}) \;=\; \binom{\lambda+x-1}{x}\Big(1-\frac{\beta}{\delta}\Big)^{\lambda}\Big(\frac{\beta}{\delta}\Big)^{x}$$

on the point $(\delta-\beta)x$ for each nonnegative integer x [33]. We shift mass from the point $(\delta-\beta)x$ to the integer x by replacing e^{-xt} in the Karlin-McGregor formula by $e^{-(\delta-\beta)xt}$. With this change made, the relevant orthogonal polynomials $q_n(x)$ are the Meixner polynomials

$$M_n(x;\lambda,\rho) \;=\; \sum_{k=0}^{n}\frac{(-n)_k(-x)_k}{(\lambda)_k k!}\left(1-\frac{1}{\rho}\right)^k$$

with $\rho = \kappa^{-1} = \beta/\delta$. Note here the use of the rising polynomial notation $(y)_k = y(y+1)\cdots(y+k-1)$. The Meixner polynomials are hypergeometric functions satisfying $M_0(x;\lambda,\rho) = 1$ and $M_n(x;\lambda,\rho) = M_x(n;\lambda,\rho)$. In view of this last property, we can write the Karlin-McGregor formula as

$$p_{mn}(t) \;=\; \pi_n\sum_{x=0}^{\infty}e^{-(\delta-\beta)xt}M_x\Big(m;\lambda,\frac{\beta}{\delta}\Big)M_x\Big(n;\lambda,\frac{\beta}{\delta}\Big)\binom{\lambda+x-1}{x}\Big(1-\frac{\beta}{\delta}\Big)^{\lambda}\Big(\frac{\beta}{\delta}\Big)^{x}.$$

Following the lead of Ismail et al. [30], we now take limits in this version of the Karlin-McGregor representation as λ tends to 0. In the limit, state 0 becomes absorbing, so $\lim_{\lambda\to 0} p_{0n}(t) = 1_{\{n=0\}}$. The case $m > 0$ is more delicate. The $x = 0$ term in our modified expansion tends to 1 when $n = 0$ and to 0 when $n > 0$. When

$x > 0$ and $n > 0$, an important part of the limit is

$$\begin{aligned}
& \lim_{\lambda \to 0} M_x\Big(n; \lambda, \frac{\beta}{\delta}\Big)\binom{\lambda + x - 1}{x} \\
= & \lim_{\lambda \to 0} \sum_{k=0}^{x} \frac{(-x)_k(-n)_k}{(\lambda)_k k!}\Big(1 - \frac{\delta}{\beta}\Big)^k \frac{(\lambda)_x}{x!} \\
= & \sum_{k=1}^{x} \frac{(-x)_k(-n)_k}{x(k-1)!k!}\Big(1 - \frac{\delta}{\beta}\Big)^k \\
= & n\Big(1 - \frac{\delta}{\beta}\Big) \sum_{k=0}^{x-1} \frac{[-(x-1)]_k[-(n-1)]_k}{k!(k+1)!}\Big(1 - \frac{\delta}{\beta}\Big)^k \\
= & n\Big(1 - \frac{\delta}{\beta}\Big) M_{x-1}\Big(n-1; 2, \frac{\beta}{\delta}\Big).
\end{aligned}$$

In the same situation,

$$\lim_{\lambda \to 0} \pi_n M_x\Big(m; \lambda, \frac{\beta}{\delta}\Big) = \frac{mx}{n}\Big(\frac{\beta}{\delta}\Big)^n \Big(1 - \frac{\delta}{\beta}\Big) M_{x-1}\Big(m-1; 2, \frac{\beta}{\delta}\Big).$$

Combining these two limits produces the expansion

$$\begin{aligned}
& \lim_{\lambda \to 0} p_{mn}(t) \\
= & m\Big(\frac{\beta}{\delta}\Big)^n \Big(1 - \frac{\delta}{\beta}\Big)^2 \sum_{x=1}^{\infty} x e^{-(\delta-\beta)xt} M_{x-1}\Big(m-1; 2, \frac{\beta}{\delta}\Big) M_{x-1}\Big(n-1; 2, \frac{\beta}{\delta}\Big)\Big(\frac{\beta}{\delta}\Big)^x
\end{aligned}$$

for $m > 0$ and $n > 0$. Finally, when $m > 0$ and $n = 0$, similar arguments yield

$$\lim_{\lambda \to 0} p_{m0}(t) = 1 + m\Big(1 - \frac{\delta}{\beta}\Big) \sum_{x=1}^{\infty} e^{-(\delta-\beta)xt} M_{x-1}\Big(m-1; 2, \frac{\beta}{\delta}\Big)\Big(\frac{\beta}{\delta}\Big)^x.$$

These representations of $p_{mn}(t)$ are convenient in studying the distribution of the number of HSCs at a random time because they depend on time only through the factors $e^{-(\delta-\beta)xt}$. Invoking the Gumbel approximation (16) to the moment generating function of the extinction time D_C of the CSCs gives

$$\mathbb{E}\left[e^{-(\delta_H - \beta_H)xD_C}\right] \approx \Big[n_C(1 - \frac{\beta_C}{\delta_C})\Big]^{-\frac{x(\delta_H - \beta_H)}{\delta_C - \beta_C}} \Gamma\Big[1 + \frac{x(\delta_H - \beta_H)}{\delta_C - \beta_C}\Big].$$

The top panel of Figure 6 shows the distribution of the number of HSCs N_H at the random extinction time of the CSCs based on the limiting eigenfunction expansions with the Gumbel approximation. Here the parameter values are $n_H = 4,400$, $\beta_H = 0.024$ week^{-1}, $\delta_H = 0.03$ week^{-1}, $n_C = 17,600$, $\beta_C = 0.024$ week^{-1}, and $\delta_C = 0.036$ week^{-1}. Smaller death rates are used for this comparison of the two methods because we were not able to obtain meaningful results from the eigenfunction expansion using higher death rates.

The eigenfunction approximation to the distribution of N_H suffers serious round-off errors when N_H is supported on a large number of points. The terms in the series are large and tend to alternate in sign. Fourier analysis offers a more numerically stable method of computing the distribution of N_H. The Fourier approach applies generically to any probability generating function $P(s) = \sum_{j=0}^{\infty} p_j s^j$ [27, 38]. To extract the coefficients of $P(s)$, extend it to the boundary of the unit circle in the complex plane via the equation $P(e^{2\pi it}) = \sum_{j=0}^{\infty} p_j e^{2\pi ijt}$, where $i = \sqrt{-1}$. This creates a periodic function in t whose kth Fourier coefficient p_k can be recovered via the finite Riemann sum

$$p_k \;=\; \int_0^1 P(e^{2\pi it}) e^{-2\pi ikt} dt \;\approx\; \frac{1}{m} \sum_{j=0}^{m-1} P(e^{2\pi ij/m}) e^{-2\pi ikj/m}.$$

In practice, one evaluates this finite Fourier transform via the fast Fourier transform algorithm for some large power m of 2. For sufficiently large m, all of the coefficients $p_0, ..., p_{m-1}$ can be computed accurately. Accuracy can be checked by comparing the numerically computed mean of $P(s)$ with its theoretical mean and variance.

To apply the Fourier method to found the distribution of N_H, let $G_H(s,t)$ and $G_C(s,t)$ be the probability generating functions of the number of HSCs and CSCs at the fixed time t. These are special cases of expression (4). Thus the generating function of the number of normal stem cells at the random time when cancer stem

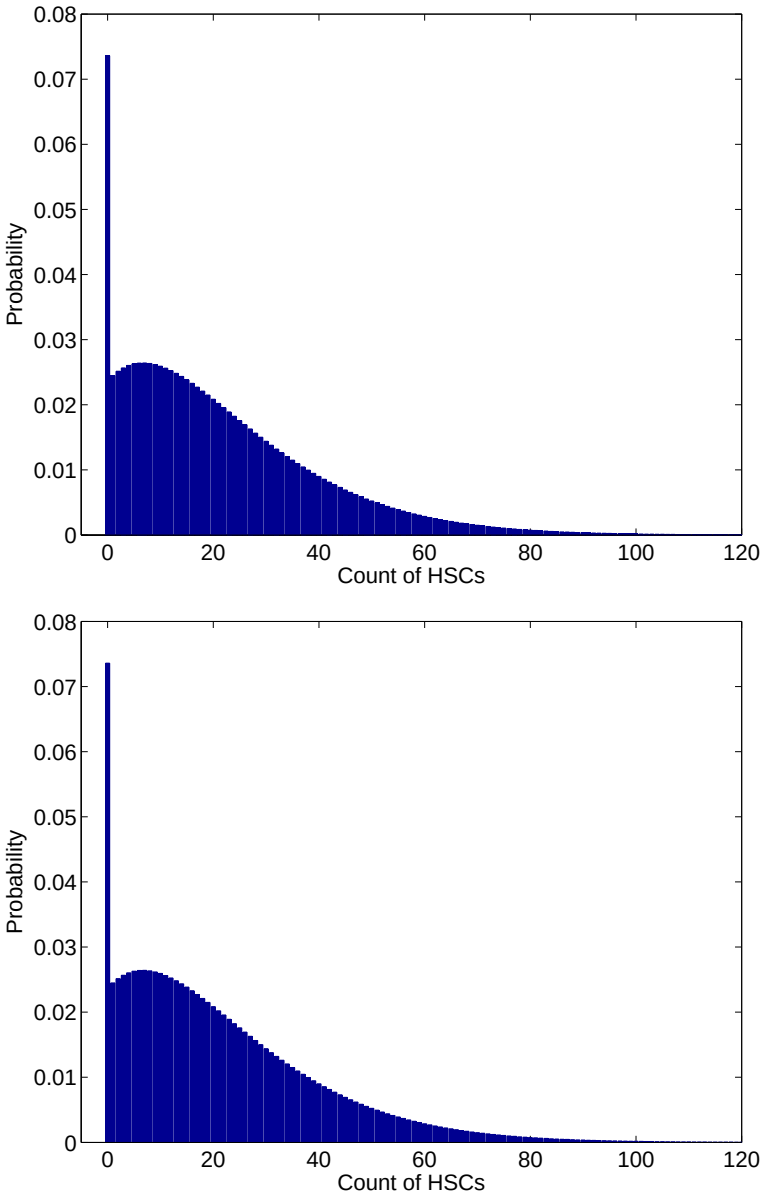

Figure 6: Comparison of two numerical methods for calculating the distribution of normal stem cells when cancer stem cells are eradicated. The parameter setting is $n_H = 4,400$, $\beta_H = 0.024$ week^{-1}, $\delta_H = 0.03$ week^{-1}, $n_C = 17,600$, $\beta_C = 0.024$ week^{-1}, and $\delta_C = 0.036$ week^{-1}. Top: Based on the Karlin-McGregor representation. Bottom: Based on the finite Fourier transform.

cells are eradicated is given by

$$G_{N_H}(s) \;=\; \int_0^\infty G_H(s,t)\frac{\partial}{\partial t}G_C(0,t)dt,$$

which can be numerically evaluated for any s, including s on the boundary of the unit circle. With this generating function at our disposal, we can retrieve the distribution of N_H by the fast Fourier transform as just explained.

The top panel of Figure 6 shows the distribution of normal cells at the random time when cancer stem cells become extinct calculated by fast Fourier transform under the same parameter settings. The numerical means and variances from both distributions match those implied by formulas (14) and (15). In the following numerical experiments, we only show the results from the more stable finite Fourier transform method. Figures 7 and 8 display the distributions of normal stem cells at fixed and random times under two typical parameter settings.

4.5 Therapy in the Presence of Quiescence

In the reversible state of quiescence, a stem cell does not divide. For many targeted therapies, the death rates of quiescent stem cells and active stem cells will be the same. Here we consider therapies that target actively dividing stem cells and largely spare quiescent stem cells. In this case, we predict that the active cancer stem cell population will be eradicated first and leave behind a quiescent cancer stem cell population, which on awakening causes recurrence of the cancer. We now present a model that validates this intuition. The model therefore highlights the danger in targeting only active cancer stem cells. For the sake of simplicity, we ignore the slow flow of active stem cells into the resting state of quiescence. We will repair this defect in Section 4.6.

Let ν be the death rate per quiescent cancer stem cell, α be rate of awakening of a quiescent cancer stem cell, and $G(t)$ be the probability that a quiescent cancer stem cell and all of its descendants have gone extinct by time t. As in the previous

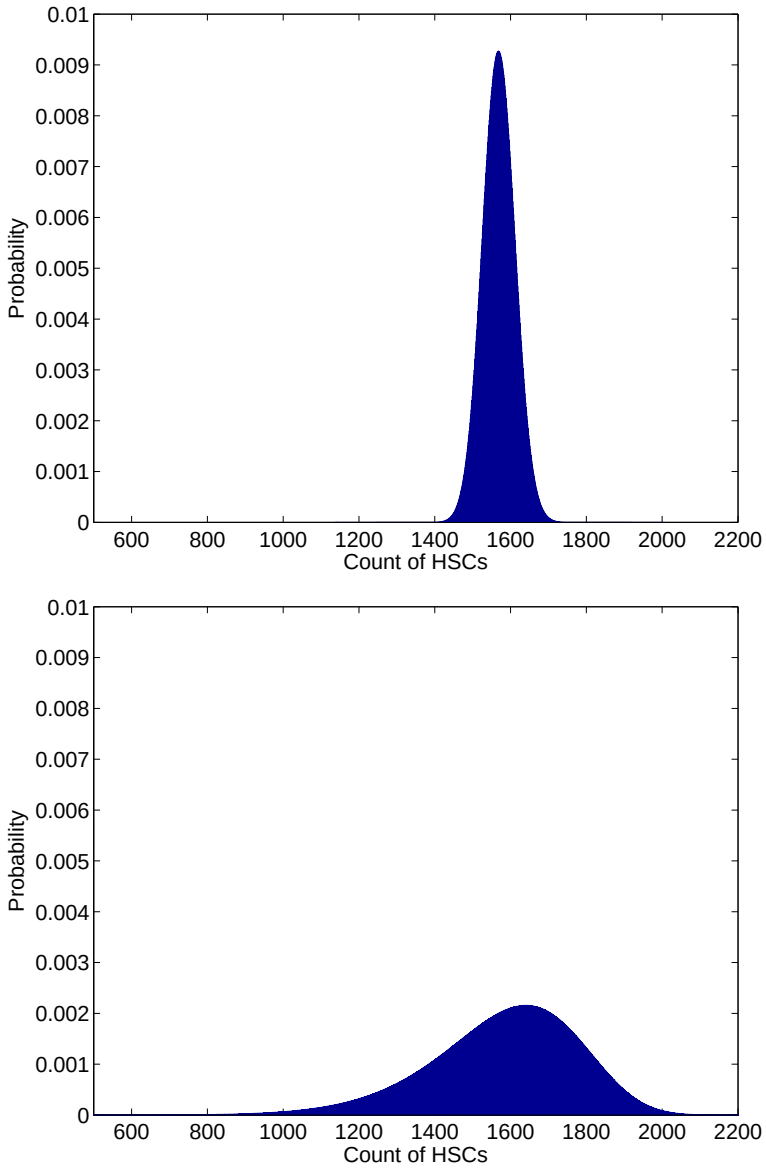

Figure 7: Distribution of HSCs when CSCs become extinct, assuming death rate of HSCs $\delta_H = 0.08$ week^{-1}. Initial clan sizes are $n_H = 4,400$ and $n_C = 17,600$, birth rates are $\beta_H = \beta_C = 0.024$ week^{-1}, and death rate of CSCs $\delta_C = 0.59$ week^{-1}. Top: Distribution at the (fixed) mean cancer extintction time 18 weeks. Bottom: Distribution at the (random) cancer extinction time.

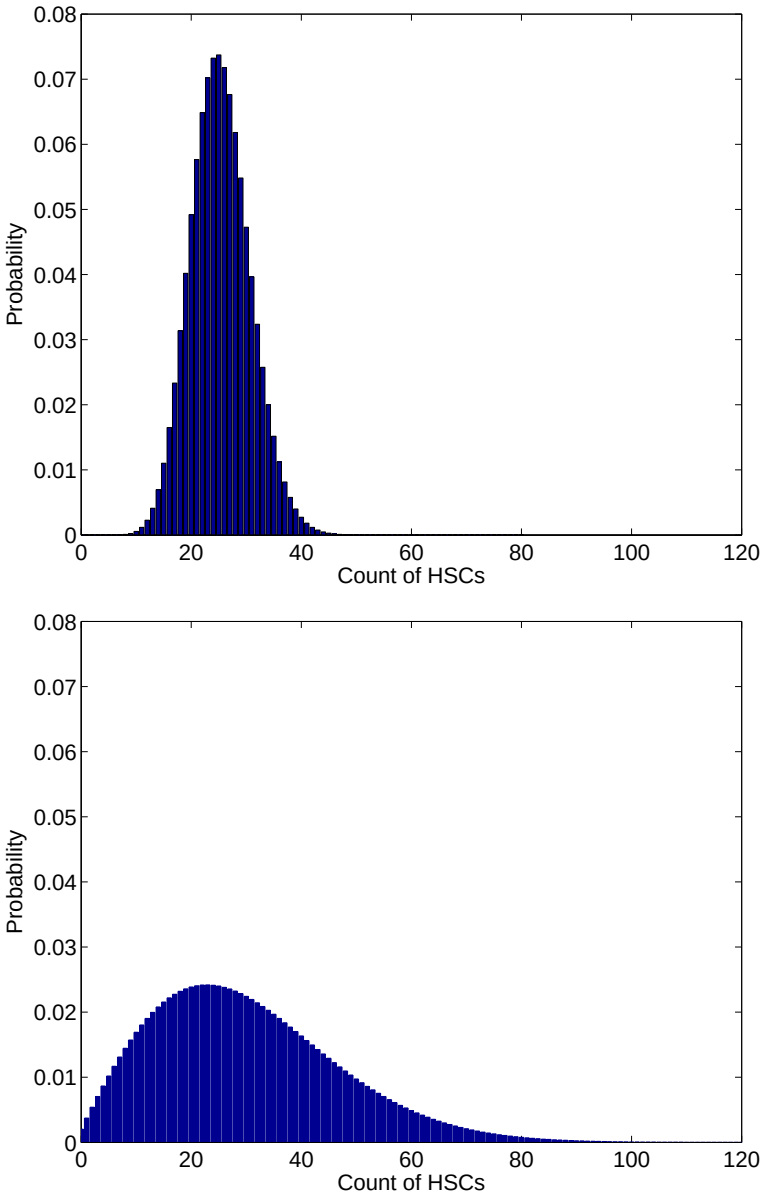

Figure 8: Distribution of HSCs when CSCs become extinct, assuming death rate of HSCs $\delta_H = 0.31$ week^{-1}. Initial clan sizes are $n_H = 4,400$ and $n_C = 17,600$, birth rates are $\beta_H = \beta_C = 0.024$ week^{-1}, and death rate of CSCs $\delta_C = 0.59$ week^{-1}. Top: Distribution at the (fixed) mean cancer extintction time 18 weeks. Bottom: Distribution at the (random) cancer extinction time.

model, β and δ are the birth and death rates, respectively, per cell for the actively dividing cancer stem cells. We begin by deriving an expression for $G(t)$. Considering the short time interval $(0, s)$, it is clear that

$$G(t+s) = [1-(\alpha+\nu)s]G(t) + \nu s + \alpha s F(t) + o(s),$$

where $F(t)$ is the extinction probability by time t starting with a single active stem cell. Sending s to 0 leads to the differential equation

$$\frac{d}{dt}G(t) = -(\alpha+\nu)G(t) + \nu + \alpha F(t).$$

with solution

$$G(t) = \frac{\nu}{\alpha+\nu}\left[1-e^{-(\alpha+\nu)t}\right] + \alpha e^{-(\alpha+\nu)t}\int_0^t e^{(\alpha+\nu)s}F(s)ds.$$

Given the identity

$$\begin{aligned}\alpha e^{-(\alpha+\nu)t}\int_0^t e^{(\alpha+\nu)s}ds &= \frac{\alpha e^{-(\alpha+\nu)t}}{\alpha+\nu}\left[e^{(\alpha+\nu)t}-1\right] \\ &= \frac{\alpha}{\alpha+\nu}\left[1-e^{-(\alpha+\nu)t}\right],\end{aligned}$$

it follows that

$$G(t) = 1 - e^{-(\alpha+\nu)t} + \alpha e^{-(\alpha+\nu)t}\int_0^t e^{(\alpha+\nu)s}\left[F(s)-1\right]ds. \tag{21}$$

In view of equation (3), we have

$$1-F(t) = \frac{(\delta-\beta)e^{(\beta-\delta)t}}{\delta-\beta e^{(\beta-\delta)t}}.$$

Substituting this in equation (21) produces

$$\begin{aligned}1-G(t) &= e^{-(\alpha+\nu)t} + \alpha e^{-(\alpha+\nu)t}\int_0^t e^{(\alpha+\nu)s}\left[1-F(s)\right]ds \\ &= e^{-(\alpha+\nu)t}\left[1+\alpha\int_0^t e^{(\alpha+\nu)s}\frac{(\delta-\beta)e^{(\beta-\delta)s}}{\delta-\beta e^{(\beta-\delta)s}}ds\right].\end{aligned}$$

Further progress can be made by exploiting the expansion

$$\frac{1}{1-\frac{\beta}{\delta}e^{(\beta-\delta)s}} = \sum_{k=0}^{\infty}\Big(\frac{\beta}{\delta}\Big)^k e^{k(\beta-\delta)s}$$

in the integral

$$\begin{aligned}\int_0^t e^{(\alpha+\nu)s}\frac{(\delta-\beta)e^{(\beta-\delta)s}}{\delta-\beta e^{(\beta-\delta)s}}ds &= \frac{(\delta-\beta)}{\delta}\int_0^t\sum_{k=0}^{\infty}\Big(\frac{\beta}{\delta}\Big)^k e^{[\alpha+\nu+(k+1)(\beta-\delta)]s}ds\\ &= \frac{(\delta-\beta)}{\delta}\sum_{k=0}^{\infty}\Big(\frac{\beta}{\delta}\Big)^k\frac{e^{[\alpha+\nu+(k+1)(\beta-\delta)]t}-1}{\alpha+\nu+(k+1)(\beta-\delta)}.\end{aligned}$$

In conclusion, we find that

$$\begin{aligned}1-G(t) &= e^{-(\alpha+\nu)t}\Big[1-\frac{\alpha(\delta-\beta)}{\delta}\sum_{k=0}^{\infty}\Big(\frac{\beta}{\delta}\Big)^k\frac{1}{\alpha+\nu+(k+1)(\beta-\delta)}\\ &\quad+\frac{\alpha(\delta-\beta)}{\delta}\sum_{k=0}^{\infty}\Big(\frac{\beta}{\delta}\Big)^k\frac{e^{[\alpha+\nu+(k+1)(\beta-\delta)]t}}{\alpha+\nu+(k+1)(\beta-\delta)}\Big].\end{aligned}\tag{22}$$

The explicit expression (22) allows us to determine the fate of a population of m cancer stem cells in quiescence. Consistent with our assumption that the killing rate δ of active cancer stem cells is much higher than the killing rate ν of quiescent cancer stem cells, we take $\alpha+\nu+\beta-\delta<0$. In this regime, formula (22) can be replaced by the approximation

$$1-G(t) = e^{-(\alpha+\nu)t}\left[1+c+o(1)\right]\tag{23}$$

where c is the positive constant

$$c = -\frac{\alpha(\delta-\beta)}{\delta}\sum_{k=0}^{\infty}\Big(\frac{\beta}{\delta}\Big)^k\frac{1}{\alpha+\nu+(k+1)(\beta-\delta)}.$$

Note that the error term $o(1)$ in (23) tends to 0 exponentially fast as t tends to ∞.

The extinction time for the last surviving clan issuing from the m initial quiescent stem cells has distribution function $G_m(t)=G(t)^m$. The asymptotic theory of

extreme order statistics also applies to $G_m(t)$. Once again we proceed by identifying a constant R such that

$$\lim_{t\to\infty} \frac{1-G(t+xR)}{1-G(t)} \;=\; e^{-x}$$

for all x. In light of the approximation (23), we have

$$\frac{1-G(t+xR)}{1-G(t)} \;=\; \frac{e^{-(\alpha+\nu)(t+xR)}\left[1+c+o(1)\right]}{e^{-(\alpha+\nu)t}\left[1+c+o(1)\right]} \;=\; e^{-(\alpha+\nu)xR}\left[1+o(1)\right],$$

and this ratio approaches e^{-x} if and only if $R=(\alpha+\nu)^{-1}$. Therefore, the previously cited extreme value theorem implies that

$$\lim_{m\to\infty} G_m(a_m+b_m t) \;=\; e^{-e^{-t}}$$

for sequences a_m and b_m defined by

$$\frac{1}{m} \;=\; 1-G(a_m) \;=\; e^{-(\alpha+\nu)a_m}\left[1+c+o(1)\right]$$

and $b_m = R = (\alpha+\nu)^{-1}$. Ignoring the error term $o(1)$, we deduce that

$$a_m \;=\; \frac{1}{\alpha+\nu}\Big[\ln m + \ln(1+c)\Big].$$

The bottom line of this analysis is that the mean time to extinction for the m quiescent cancer stem cells is approximately

$$\frac{1}{\alpha+\nu}\Big[\ln m + \ln(1+c)\Big] + \frac{\gamma}{\alpha+\nu}. \tag{24}$$

On the other hand, the mean extinction time for the n active cancer stem cells is

$$\frac{1}{\delta-\beta}\Big[\ln n + \ln\Big(\frac{\delta-\beta+\frac{\beta}{n}}{\delta}\Big)\Big] + \frac{\gamma}{\delta-\beta}. \tag{25}$$

Our assumption $\alpha+\nu<\delta-\beta$ is equivalent to $(\delta-\beta)^{-1}<(\alpha+\nu)^{-1}$. Thus, unless n is much larger than m, the active cancer stem cells go extinct before the quiescent cancer stem cells. This is the opposite of what a viable therapy should achieve.

4.6 Distribution of HSCs in the Presence of Quiescence

Instead of ignoring flow into the quiescent state, one can incorporate it as part of a comprehensive branching process model [12]. We now briefly sketch this model. Consider a two-type branching process with quiescent cells as type 1 particles and active cells as type 2 particles. In addition to the notation of the previous section, let ϕ be the rate per cell of falling into quiescence. In a branching process, a particle reproduces at the time of its death. Let f_{ij} be the mean number of daughter particles of type j that a type i particle produces. Straightforward reasoning determines the reproduction matrix $F = (f_{ij})$ in our model as

$$F = \begin{pmatrix} 0 & \frac{\alpha}{\alpha+\nu} \\ \frac{\phi}{\phi+\beta+\delta} & \frac{2\beta}{\phi+\beta+\delta} \end{pmatrix}.$$

Other key ingredients are the death rates per particle. These can be summarized by the vector ψ with components $\psi_1 = \alpha + \nu$ and $\psi_2 = \phi + \beta + \delta$. These constructs determine a matrix $M(t)$ whose typical entry $m_{ij}(t)$ equals the mean number of particles of type j at time t starting with a single particle of type i at time 0. Again standard arguments show that $M(t) = e^{t\Omega}$, where $\Omega = [\psi_i(f_{ij} - 1_{\{i=j\}})]$. Similar but more complicated reasoning yield the variance-covariance matrix of the particle counts starting from any initial configuration of particles [12].

To capture the full distribution of particle counts at a future time, it is convenient to introduce a bivariate generating function $P_i(t, \mathbf{z})$ for the joint particle counts at time t starting from a single particle of type i at time 0. In our model, the backward differential equations for these two generating functions amount to

$$\begin{aligned} \frac{\partial}{\partial t} P_1(t, \mathbf{z}) &= -(\alpha + \nu) P_1(t, \mathbf{z}) + \nu + \alpha P_2(t, \mathbf{z}) \\ \frac{\partial}{\partial t} P_2(t, \mathbf{z}) &= -(\phi + \beta + \delta) P_2(t, \mathbf{z}) + \delta + \phi P_1(t, \mathbf{z}) + \beta P_2(t, \mathbf{z})^2 \end{aligned}$$

with initial condition $P_i(0, \mathbf{z}) = z_i$. The probability of extinction by time t equals $P_1(t, \mathbf{0})^{n_1} P_2(t, \mathbf{0})^{n_2}$, where n_i is the number of type i particles at time 0. Although

it is impossible to solve for $P_1(t, \mathbf{z})$ and $P_2(t, \mathbf{z})$ analytically, it is certainly possible to solve for them numerically for any fixed value of $\mathbf{z}$. This suggests retrieving the bivariate distributions via the 2D fast Fourier transform. In practice, this procedure works well and gives means and variances closely approximating the theoretical means and variances. Extension to the kind of random times we have stressed is feasible. Figure 9 displays some typical results, for the parameter choices: $\beta_H = \beta_C = 0.024$ week^{-1}, $\delta_C = 0.59$ week^{-1}, $\delta_H = 0.08$ week^{-1}, $\nu_H = \nu_C = 0.00024$ week^{-1}, $\phi_C = \phi_H = 0.007$ week^{-1}, and $\alpha_C = \alpha_H = 0.07$ week^{-1}. Here we show the distribution of quiescent and active CSCs at the fixed mean extinction time of active CSCs, as estimated from equation (25), and the distribution of HSCs at the mean extinction time of quiescent CSCs, as estimated from equation (24). Finally, we show the distribution of HSCs at the random time of extinction of both quiescent and active CSCs.

5 Stochastic Simulation

Because branching process models resist full mathematical analysis, progress depends on a variety of numerical tools. Unfortunately, as model complexity increases, all known deterministic numerical methods falter under the overwhelming computational loads. At this point simulation becomes an attractive alternative. Simulation has the further virtue of simplicity of implementation. Even when better tools are available, simulation promotes rapid testing of models and checking of approximate solutions. For these reasons, we now describe our experience with stochastic simulation in the stem cell model.

Recent advances in stochastic simulation are geared to the study of continuous-time Markov chains with a finite number of particle types, interacting via a finite number of reaction channels. While the methods first described by Gillespie [18, 19] were rooted in applications to chemical reaction kinetics, particle-based stochastic

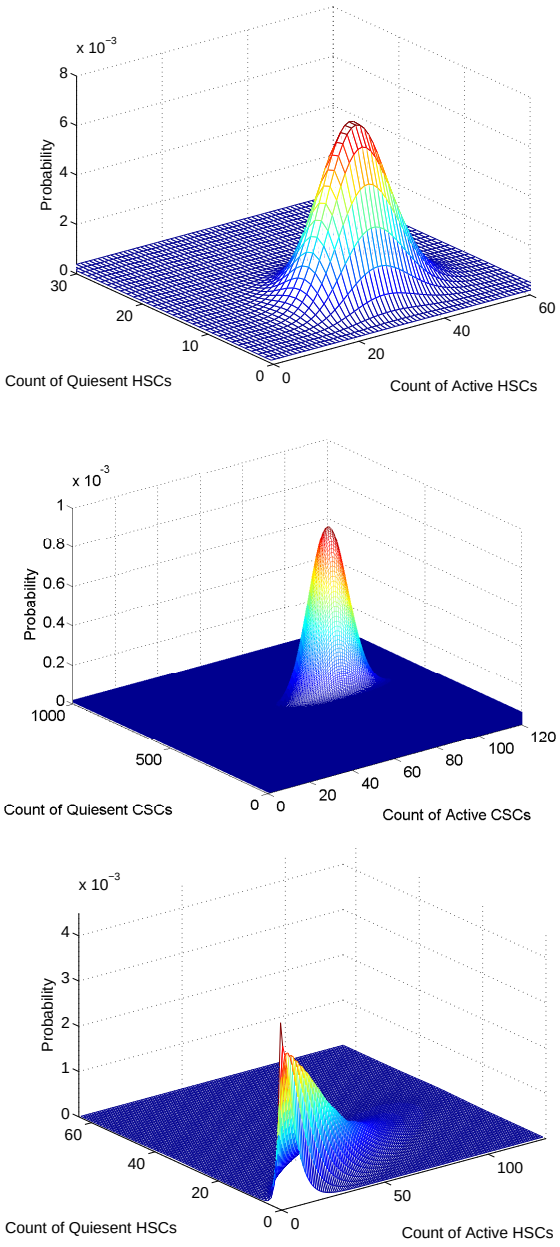

Figure 9: Dynamics of quiescent and active HSCs and CSCs at fixed and random extinction times. Top: Distribution of HSCs remaining at the mean extinction time of quiescent CSCs (114 weeks). Middle: Distribution of CSCs at the mean extinction time of active CSCs (18 weeks). Bottom: Distribution of HSCs at the random time of CSC extinction.

simulation models have broad applications in fields as diverse as queuing theory, population dynamics, gene regulation, and biochemical networks [28, 60]. The stochastic simulation algorithm (SSA) employs a wait and jump mechanism to simulate the behavior of a chain. Because it simulates every reaction, SSA can be annoyingly slow in models with large particle counts. The τ-leaping method [7, 20] leaps over intermediate events by taking a fixed time step of length τ, chosen so that all reaction propensities (intensities) are relatively constant during the leap interval. At the end of the interval, each reaction channel fires a Poisson number of times with mean determined by the product of its propensity and τ. The τ-leaping method trades small losses in accuracy for much larger time steps. Our recent step anticipation leaping (SAL) method [53] generalizes τ-leaping by projecting linear and quadratic changes in reaction propensities. This promotes better accuracy without compromising speed. Here we employ the SAL method to explore stem cell dynamics in both the presence and absence of quiescence. The simulations substantiate our previous analytic and numerical results.

In a continuous-time Markov chain with a finite number of particle types, let X_t be the particle count vector at time t, r_j be the propensity of reaction j, and ϵ^j be the increment to X_t caused by the firing of reaction j. The τ-leaping method runs an independent Poisson process for each reaction channel and sums the results over short time intervals. In ordinary τ-leaping, reaction channel j will fire $r_j\tau$ times on average during $(t, t+\tau)$. One therefore updates the particle count vector $X_t = x$ by the sum $X_{t+\tau} = x + \sum_j N_j\epsilon^j$, where N_j are independent Poisson variates with means $r_j\tau$. In SAL, we expand each propensity to first order, replacing the constant intensity r_j of ordinary τ-leaping by the linear intensity

$$r_j(X_{t+s}) \approx r_j(X_t) + \frac{d}{dt} r_j(X_t)s.$$

Under this approximation, reactions of type j occur according to an inhomogeneous

Poisson process during $(t, t+\tau)$, and the mean number of reactions is

$$\omega_j(t, t+\tau) \;=\; \int_0^\tau \left[r_j(X_t) + \frac{d}{dt} r_j(X_t) s \right] ds \;=\; r_j(X_t)\tau + \frac{d}{dt} r_j(X_t) \frac{1}{2}\tau^2.$$

This raises the question of how to calculate the derivative $\frac{d}{dt} r_j(x)$. The most natural route uses the chain rule

$$\frac{d}{dt} r_j(x) \;=\; \sum_{k=1}^{d} \frac{\partial}{\partial x_k} r_j(x) \frac{d}{dt} x_k$$

and sets

$$\frac{d}{dt} x_k \;=\; \sum_{j=1}^{c} r_j(x) \epsilon_k^j, \tag{26}$$

where ϵ_k^j is the increment to species k caused by reaction j. The reaction rate equation (26) models the mean behavior of the system when particle counts are high and stochastic fluctuations can be ignored. The following examples employ linear SAL. Quadratic extrapolation is possible, but the improvements over linear extrapolation are rather modest [53].

Empirical Distribution of HSCs When CSCs Go Extinct

In our basic model without quiescence, there are 2 populations of cells and 4 reaction channels. The Markov chain X_t has component X_{t1} counting the CSCs and component X_{t2} counting the HSCs. Table 1 lists the reaction channels, propensities, and reaction increments. Here ϵ_j^k indicates the change in species k under reaction j. Any unspecified ϵ_j^k is assumed to be 0.

Stochastic simulation allows us to explore the distribution of the number N_H of HSCs at the random time of extinction of the CSCs; we simply record the number of HSCs when the CSC count reaches 0. Figure 10 shows the distribution of N_H over 10,000 SAL trials for the two values $\delta_H = 0.08$ week^{-1} and $\delta_H = 0.31$ week^{-1}.

Reaction	Propensity	Increment Vector
CSC birth	$\beta_C x_1$	$\epsilon_1^1 = +1$
CSC death	$\delta_C x_1$	$\epsilon_1^2 = -1$
HSC birth	$\beta_H x_2$	$\epsilon_2^3 = +1$
HSC death	$\delta_H x_2$	$\epsilon_2^4 = -1$

Table 1: Simulation of CSCs and HSCs under therapy.

The other reaction rates $\beta_C = \beta_H = 0.024$ week^{-1} and $\delta_C = 0.59$ week^{-1} match our earlier choices.

These results highlight the dependence of N_H on the selectivity σ of therapy. In the top panel of Figure 10, with selectivity $\sigma = 10$, there is very little chance that the population of HSCs goes extinct before all CSCs are eradicated. By contrast, in the bottom panel of Figure 10, with selectivity $\sigma = 2$, there is a good chance that HSCs go extinct before CSC eradication. The random variable N_H has mean $\pm$ one standard deviation of $1,580 \pm 198$ for $\sigma = 10$ and 30.0 ± 17.1 for $\sigma = 2$. These results agree well with our analytic formulas and numerical results based on the finite Fourier transform.

Simulations in the Presence of Quiescence

When we introduce quiescence into the model, we have 4 populations of cells: active CSCs (type 1) and HSCs (type 2) and quiescent CSCs (type 3 or qCSC) and HSCs (type 4 or qHSC). Table 2 lists the reactions, propensities, and increment vectors of the extended model.

Because the deaths of quiescent cells, both qCSCs and qHSCs, are rare events, we set $\nu_C = \nu_H = 0.00024$ week^{-1}. To deduce the relative rates of awakening and falling into quiescence, consider a simple 2-state Markov chain ignoring birth and death and modeling only the passage of a single stem cell back and forth between the active

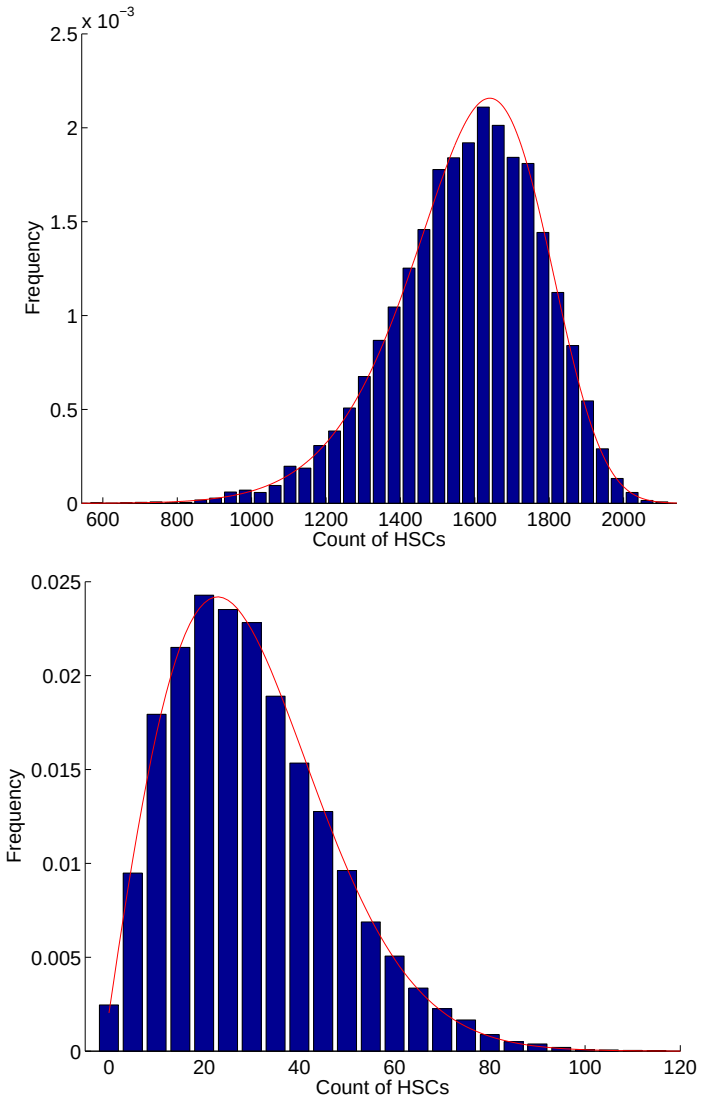

Figure 10: Distribution of the number of HSCs at the random time of CSC extinction. Solid bars represent results obtained using stochastic simulation, while lines represent results obtained using finite Fourier transform. Top: $\delta_H = 0.08$ week^{-1}, $\sigma = 10$. Bottom: $\delta_H = 0.31$ week^{-1}, $\sigma = 2$.

Reaction	**Propensity**	**Increment Vector**
CSC birth	$\beta_C x_1$	$\epsilon_1^1 = +1$
CSC death	$\delta_C x_1$	$\epsilon_1^2 = -1$
CSC quiescence	$\phi_C x_1$	$\epsilon_1^3 = -1$, $\epsilon_3^3 = +1$
qCSC awakening	$\alpha_C x_3$	$\epsilon_1^4 = +1$, $\epsilon_3^4 = -1$
qCSC death	$\nu_C x_3$	$\epsilon_3^5 = -1$
HSC birth	$\beta_H x_2$	$\epsilon_2^6 = +1$
HSC death	$\delta_H x_2$	$\epsilon_2^7 = -1$
HSC quiescence	$\phi_H x_2$	$\epsilon_2^8 = -1$, $\epsilon_4^8 = +1$
qHSC awakening	$\alpha_H x_4$	$\epsilon_2^9 = +1$, $\epsilon_4^9 = -1$
qHSC death	$\nu_H x_4$	$\epsilon_4^{10} = -1$

Table 2: Simulation with quiescence and awakening

and quiescent states. This chain is reversible, and the principle of detailed balance identifies $\pi = \alpha/(\phi + \alpha)$ as the equilibrium fraction of active stem cells. Based on observations in adult mice that approximately 75 % of long-term self-renewing hematopoietic stem cells are quiescent [9], and observations in patients with chronic myelogenous leukemia that 8.7 % of CD34 cells are in a quiescent state [29], we take $\pi_H = 0.25$ and $\pi_C = 0.9$. While no data are available on rates of activation and quiescence of stem cells, we start with activation rates $\alpha_H = \alpha_C = 0.07$ week^{-1}, and calculate the rates of quiescence $\phi_H = 0.21$ week^{-1} and $\phi_C = 0.007$week^{-1} using the detailed balance condition. Given a total stem cell population size of $22,000$ [1], we again start with a large proportion (80%) of CSCs: $n_H = 4,400$ HSCs and $n_C = 17,600$ CSCs. Based on the above proportions of quiescent and active HSCs and CSCs, the initial value $X_0 = x$ has components $x_1 = 15,840$, $x_2 = 1,100$, $x_3 = 1,760$, and $x_4 = 3,300$.

We will consider two cases. The first assumes a slow backflow to quiescence ($\phi_C = \phi_H = 0.007$ week^{-1}). This scenario may be more realistic as quiescence is most likely regulated by similar mechanisms for both types of cells, and healthy stem

cells might be expected to spend more time in an active state during malignancy. The second scenario is less likely and assumes that the CSCs and HSCs have reached two different equilibrium distributions. Here the backflow of quiescence is slow for CSCs ($\phi_C = 0.007$ week^{-1}) and fast for HSCs ($\phi_H = 0.21$ week^{-1}). We use our previous birth rates $\beta_H = \beta_C = 0.024$ week^{-1} and death rates $\delta_C = 0.59$ week^{-1} and $\delta_H = 0.08$ week^{-1}.

Following the trajectories of the 4 populations of stem cells over time in Figure 11, we see it takes a much longer time for the CSCs to go extinct when quiescence is involved (t= 40 weeks). When the backflow to quiescence is much slower for CSCs ($\phi_C = 0.007$ week^{-1}; $\phi_H = 0.21$ week^{-1}), there is still an adequate number of HSCs at the time of extinction of the CSCs, approximately 590 (124 active and 466 quiescent), though far fewer than if therapy were to target quiescent CSCs. However, when backflow to quiescence is slow for both CSCs and HSCs, $\phi_C = \phi_H = 0.007$ week^{-1}, by the time all CSCs are finally eradicated, there are only approximately 18 HSCs (13 active and 5 quiescent). In the second scenario, quiescence serves as a sanctuary for the HSCs. The first scenario agrees with the analytic results of our modeling described in Section 4.5 and emphasizes the need for therapy to target both active and quiescent CSCs. The second scenario hints at greater subtlety and emphasizes the need for accurate measurement of all parameters.

6 Conclusions

Cancer therapy based on eradicating CSCs is admittedly speculative. However, given the toll of mortality and morbidity exacted by cancer, this is a strategy worth considering in detail. Mathematical models can guide the rational design of drugs and treatments. Of course, model predictions will have to checked by animal experiments and careful analysis of patient outcomes. Premature trials with poor outcomes can sour the prospects of even a good therapy. Our findings are cause for

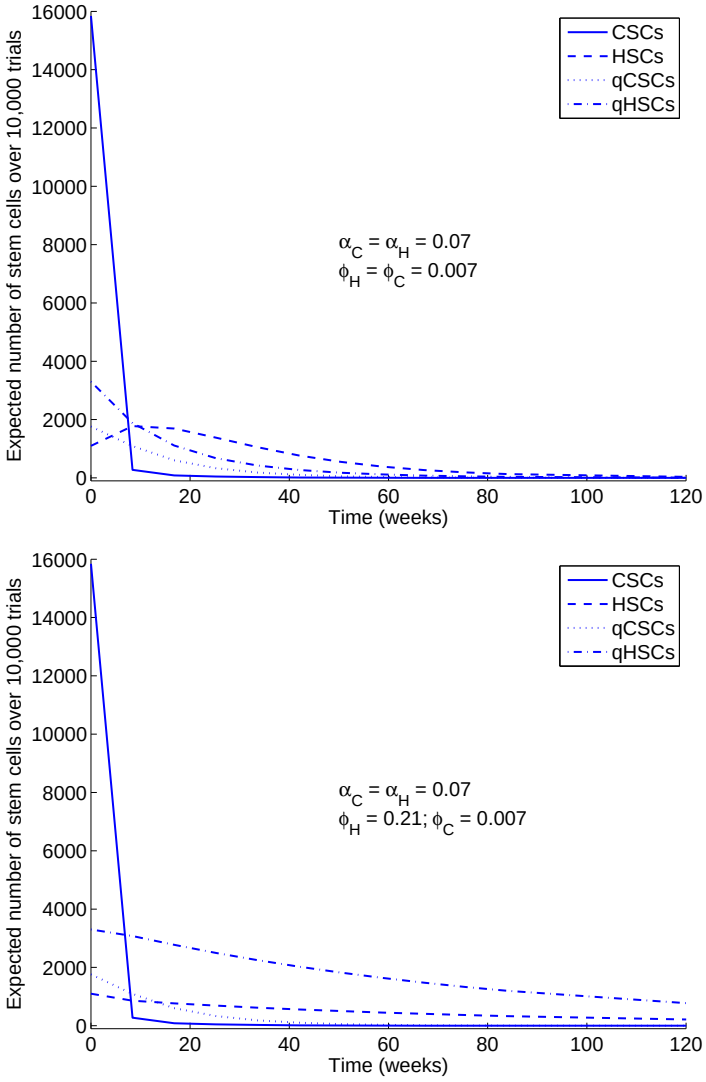

Figure 11: Trajectories of active and quiescent stem cell populations. Top: Same quiescence rates for CSCs and HSCs. Bottom: Quiescence rate for HSCs >> quiescence rate for CSCs.

guarded optimism. We have shown that the relative numbers of CSCs and HSCs at the time of initiating therapy are less relevant than the selectivity of therapy. Modeling stem cell population dynamics as a birth-death process permits characterization of the extinction times for active and quiescent stem cells and calculation of the distribution of the number of HSCs at the time of eradication of CSCs. We anticipate that comparing *in vitro* killing rates of CSCs and HSCs will be useful in screening targeted therapies. How applicable the models will be depends on underlying parameters such as absolute quantities of stem cells, death rates of HSCs and CSCs, and relative rates of quiescence and awakening. These parameters will doubtless vary for different tumor types and stem cell populations.

Cancer modeling is becoming more of a preoccupation for applied mathematicians. The variety of approaches is impressive. These range from continuum mechanics models of tumor growth to reaction-diffusion models of tumor vascularization and optimization of radiation doses in radiation therapy [3, 8, 17, 54]. Branching processes and continuous-time Markov chain models have long provided quantitative insights into the dynamics of cancer initiation and proliferation [36, 39]. Our stem cell models continue in this tradition. In stem cell dynamics, the population of HSCs is critically small, and their chance elimination has devastating consequences. This sober fact highlights the importance of tight control over killing differentials. Stochastic models of drug resistance of stem cells have also been explored [21, 37, 44]. Here modeling mutation is crucial. Further research is surely merited on the mutational pathways leading to cancer, the genetic instability of cancer stem cells, the development of resistance mutations during therapy, and the role of the stem cell niche in regulating stem cell and progenitor expansion.

We predict that stochastic simulation methods will play an increasing role in the development of more sophisticated cancer models. Stochastic simulation is ideal for studying complex systems with multiple cellular species tied together by multiple

reaction channels. We have modeled sensitivity to therapy by varying death rates. To capture the role of the stem cell niche, one could assign CSCs that escape niche regulation higher birth rates or higher rates of awakening from quiescence. We have omitted progenitor cells and partially and fully differentiated cells from our models. Adding all of the complications requires flexible modeling tools. Multitype branching processes can take us only so far. As soon as the different cell types begin to interact, the branching process paradigm breaks down. This should not mean the abandonment of stochastic models, but it does put a premium on the development of faster, more accurate, and more convenient implementations of stochastic simulation. These urgent needs and the burgeoning of systems biology as a whole will drive the field of stochastic simulation.

In conclusion, mathematical modeling and the development of rational stem cell therapy will go hand in hand. The current stem cell models give us hope that attacking CSCs can cure cancer. To be successful, targeted therapies must be tuned to spare HSCs and eradicate quiescent as well as active CSCs. This second criterion rules out drugs that solely attack dividing cells. Only stochastic models can capture the extinction and small numbers phenomena connected with stem cells. These models will ultimately provide the same extraordinary insight into cancer therapy responses and resistance that they have in HIV treatment [11]. If we are fortunate, models of the two diseases will cross fertilize each other for years to come.

Acknowledgments. We would like to thank Dr. Elliot Landaw, Dr. Van Savage, and Lindsay Riley for helpful comments and suggestions on this manuscript. This research was supported in part by USPHS grants GM53275 and MH59490 and NIH service award GM008185, and by a Young Investigator Award from the American Society of Clinical Oncology.

References

[1] J.L. Abkowitz, S.N. Catlin, M.T. McCallie, P. Guttorp, *Evidence that the number of hematopoietic stem cells per animal is conserved in mammals,* Blood, 100 (2002), pp. 2665–2667.

[2] M. Al-Hajj, M.S. Wicha, A. Benito-Hernandez, et al., *Prospective identification of tumorigenic breast cancer cells,* Proc. Natl. Acad. Sci. USA, 100 (2003), pp. 3983–3988.

[3] D. Ambrosi, and F. Mollicab, *On the mechanics of a growing tumor,* Int. J. Eng. Sci., 40 (2002), pp. 1297–1316.

[4] S. Bao, Q. Wu, R.E. McLendon, et al. *Glioma stem cells promote radioresistance by preferential activation of the DNA damage response,* Nature, 444 (2006), 756–760.

[5] S. Bao, *Targeting cancer stem cells through L1CAM suppresses glioma growth,* Cancer Res., 68 (2008), pp. 6043–6048.

[6] D. Bonnet, *Haematopoietic stem cells,* J. Pathol., 197 (2002), pp. 430–440.

[7] Y. Cao, D.T. Gillespie, and L.R. Petzold, *Efficient step size selection for the tau-leaping simulation method,* J. Chem. Phys., 124 (2006), pp. 1–11.

[8] J.J. Casciari, S.V. Sotirchos, and R.M. Sutherland, *Variations in tumor cell growth rates and metabolism with oxygen concentration, glucose concentration, and extracellular pH,* J. Cell. Physiol., 151 (1992), pp. 386–394.

[9] S.H. Cheshier, S.J. Morrison, X. Liao, and I.L. Weissman, *In vivo proliferation and cell cycle kinetics of long-term self-renewing hematopoietic stem cells,* Proc. Natl. Acad. Sci. USA, 96 (1999), pp. 3120–3125.

[10] C.V. Cox, R.S. Everly, A. Oakhill, et al., *Characterization of acute lymphoblastic leukemia progenitor cells,* Blood, 104 (2004), pp. 2919–2925.

[11] K.S. Dorman, A.H. Kaplan, K.L. Lange, and J.S. Sinsheimer, *Mutation Takes No Vacation: Can Structured Treatment Interruptions Increase the Risk of Drug-Resistant HIV-1?* , J. Acquir. Immune Defic. Syndr., 25 (2000), pp. 398–402.

[12] K. Dorman, J.S. Sinsheimer, and K. Lange, *In the garden of branching processes,* SIAM Rev., 46 (2004), pp. 222–229.

[13] K. El-Shami, and B.D. Smith, *Immunotherapy for myeloid leukemias: current status and future directions,* Leukemia, 22 (2008), pp. 1658–64.

[14] W. Feller, *An Introduction to Probability Theory and Its Applications,* John Wiley & Sons, Inc., New York, 1968.

[15] T.S. Ferguson, *A Course in Large Sample Theory,* Chapman & Hall/CRC, New York, 1996.

[16] P.J. Fialkow, R.J. Jacobson, and T. Papayannopoulou, *Chronic myelocytic leukemia: clonal origin in a stem cell common to the granulocyte, erythrocyte, platelet and monocyte/macrophage,* Am. J. Med., 63 (1977), pp.125–130.

[17] R.A. Gatenby, and E.T. Gawlinski, E.T., *A reaction-diffusion model of cancer invasion,* Cancer Res., 56 (1996), pp. 5745–5753.

[18] D.T. Gillespie, *A general method for numerically simulating the stochastic time evolution of coupled chemical reactions,* J. Comput. Phys., 22 (1976), pp. 403–434.

[19] D.T. Gillespie, *Exact stochastic simulation of coupled chemical reactions,* J. Phys. Chem., 81 (1977), pp. 2340–2361.

[20] D.T. Gillespie, *Approximate accelerated stochastic simulation of chemically reacting systems,* J. Chem. Phys., 115 (2001), pp. 1716–1733.

[21] J.H. Goldie, and A.J. Coldman,, *Quantitative model for multiple levels of drug resistance in clinical tumors,* Cancer Treat Rep., 67 (1983), 923–931.

[22] R.L. Graham, D.E. Knuth, and O. Patashnik, *Concrete Mathematics,* Addison-Wesley Publishing Company, Menlo Park, CA, 1989.

[23] G.R. Grimmett, and D.R. Stirzaker, *Probability and Random Processes,* Clarendon Press, Oxford, 1992.‘

[24] M.L. Guzman, R.M. Rossi, and L. Karnischky, *The sesquiterpene lactone parthenolide induces apoptosis of human acute myelogenous leukemia stem and progenitor cells,* Blood, 105 (2005), pp. 4163–4169.

[25] T.E. Harris, *The Theory of Branching Processes,* Dover Publications, Inc., New York, 1989.

[26] L. Hayflick, *The limited in vitro lifetime of human diploid cell strains,* Exp. Cell Res. 37 (1965), pp. 614–636.

[27] P. Henrici, *Fast Fourier methods in computational complex analysis*, SIAM Rev., 21 (1979), pp. 481–527.

[28] D.J. Higham, *Modeling and simulating chemical reactions,* SIAM Rev., 50 (2008), pp. 347–368.

[29] T.L. Holyoake, X. Jiang, H.G. Jorgensen, et al., *Primitive quiescent leukemic cells from patients with chronic myeloid leukemia spontaneously ini-*

tiate factor-independent growth in vitro in association with up-regulation of expression of interleukin-3, Blood, 97 (2001), pp. 720–728.

[30] M.E.H. Ismail, J. Letessier, and G. Valent, *Birth and death processes with absorption,* Internat. J Math. & Math. Sci., 15 (1992), pp. 469–480.

[31] C.H. Jamieson, L.E. Ailles, S.J. Dylla, et al., *Granulocyte-macrophage progenitors as candidate leukemic stem cells in blast-crisis CML,* N. Engl. J. Med., 351 (2004), pp. 657–667.

[32] S.S. Karhadkar, G.S. Bova, N. Abdallah, et al., *Hedgehog signalling in prostate regeneration, neoplasia and metastasis,* Nature, 431 (2004), 707–712.

[33] S. Karlin, and J. McGregor, *Linear growth birth and death processes,* J. Math. Mech., 7 (1958), pp. 643–662.

[34] S. Karlin, and H. Taylor, *A First Course in Stochastic Processes,* Elsevier, San Diego, 1975.

[35] E. Kavalerchik, D. Goff, and C.H.M. Jamieson, *Chronic myeloid leukemia stem cells,* J. Clin. Oncol., 26 (2008), pp. 2911–2915.

[36] M. Kimmel, and D.E. Axelrod, *Branching Processes in Biology,* Springer-Verlag, New York, 2002.

[37] N.L. Komarova, and D. Wodarz, *Drug resistance in cancer: principles of emergence and prevention,* Proc. Natl. Acad. Sci. USA, 102 (2005), pp. 9714–9719.

[38] K.L. Lange, *Numerical Analysis for Statisticians,* Springer-Verlag, New York, 1999.

[39] K.L. Lange, *Applied Probability,* Springer-Verlag, New York, 2003.

[40] T. Lapidot, C. Sirard, J. Vormoor, et al., *A cell initiating human acute myeloid leukaemia after transplantation into SCID mice,* Nature, 367 (1994), pp. 645–648.

[41] R. Liu, X. Wang, G.Y. Chen, et al. *The prognostic role of a gene signature from tumorigenic breast cancer cells,* N. Engl. J. Med., 356 (2007), 217–226.

[42] J.A. Martinez-Agosto, H.K.A. Mikkola, V. Hartenstein, AND U. Banerjee, *The hematopoietic stem cell and its niche: a comparative view,* Genes Dev., 21 (2007), pp. 3044–3060.

[43] W. Matsui, C.A. Hugg, Q. Wang, et al., *Characterization of clonogenic multiple myeloma cells,* Blood, 103 (2004), pp. 2332–2336.

[44] F. Michor, T.P. Hughes, Y. Iwasa, S. Branford, N.P. Shah, C.L. Sawyers, and M.A. Nowak, M.A., *Dynamics of chronic myeloid leukaemia,* Nature, 435 (2005), pp. 1267–1270.

[45] C.A. O'Brien, A. Pollett, S. Gallinger, et al., *A human colon cancer cell capable of initiating tumour growth in immunodeficient mice,* Nature, 445 (2007), pp. 106–110.

[46] O.K. Okamoto, and J.F. Perez, *Targeting cancer stem cells with monoclonal antibodies: a new perspective in cancer therapy and diagnosis,* Expert Rev. Mol. Diagn., 8 (2008), pp. 387–393.

[47] C.L. Olsen, P.P. Hsu, J. Glienke, et al., *Hedgehog-interacting protein is highly expressed in endothelial cells but down-regulated during angiogenesis and in several human tumors,* BMC Cancer, 4 (2004), pp. 43.

[48] R. Pardal, M.F. Clarke, and S.J. Morrison, *Applying the principles of stem-cell biology to cancer,* Nat. Rev. Cancer, 3 (2003), pp. 895–902.

[49] M.E. Prince, R. Sivanandan, A. Kaczorowski, et al., *Identification of a subpopulation of cells with cancer stem cell properties in head and neck squamous cell carcinoma,* Proc. Natl. Acad. Sci. USA, 104 (2007), 973–978.

[50] T. Reya, S.J. Morrison, M.F. Clarke, and I.L. Weissman, *Stem cells, cancer, and cancer stem cells,* Nature, 414 (2001), pp. 105–111.

[51] Y. Ruzankina, C. Pinzon-Guzman, A. Asare, et al., *Deletion of the developmentally essential gene ATR in adult mice leads to age-related phenotypes and stem cell loss,* Cell Stem Cell., 1 (2007), pp. 113–126.

[52] T. Schatton, G.F. Murphy, N.Y. Frank, et al., *Identification of cells initiation human melanomas,* Nature, 451 (2008), pp. 345–349.

[53] M.E. Sehl, A.L. Alekseyenko, K.L. Lange, *Accurate stochastic simulation via the step anticipation τ-leaping (SAL) algorithm,* J. Comput. Biol., *in press.*

[54] D.M. Shepard, M.C. Ferris, G.H. Olivera, and T.R. Mackie, T.R., *Optimizing the delivery of radiation therapy to cancer patients,* SIAM Rev., 41 (1999), 721–744.

[55] I. Shih, and T. Wang, *Notch signaling, γ-secretase inhibitors, and cancer therapy,* Cancer Res., 67 (2007), pp. 1879–1882.

[56] S.K. Singh, C. Hawkins, I.D. Clarke, et al., *Identification of human brain tumour initiating cells,* Nature, 432 (2004), pp. 396–401.

[57] M. Suva, N. Riggi, J. Stehle, et al., *Identification of cancer stem cells in Ewing's sarcoma,* Cancer Res., 69 (2009), pp. 1776–1781.

[58] J.C. Wang, T. Lapidot, J.D. Cashman, et al., *High level engraftment of NOD/SCID mice by primitive normal and leukemic hematopoietic cells from*

patients with chronic myeloid leukemia in chronic phase, Blood. 91 (1998), pp. 2406–2414.

[59] M.S. Wicha, S. Liu, and G. Dontu, *Cancer stem cells: An old idea – a paradigm shift,* Cancer Res., 66 (2006), pp. 1883–1890.

[60] D.J. Wilkinson, *Stochastic Modelling for Systems Biology,* Chapman & Hall/CRC, Boca Raton, FL, 2006.

[61] L. Xin, D.A. Lawson, and O.N. Witte, *The Sca-1 cell surface marker enriches for a prostate-regenerating cell sub-population that can initiate prostate tumorigenesis,* Proc. Natl. Acad. Sci. USA, 102 (2005), pp. 6942–6947.

[62] O.H. Yilmaz, R. Valdez, B.K. Theisen, W. Guo, D.O. Ferguson, H. Wu, and S.J. Morrison, *Pten dependence distinguishes haematopoietic stem cells from leukaemia-initiating cells,* Nature, 441 (2006), pp. 475–82.

[63] O.H. Yilmaz, and S.J. Morrison, *The PI-3kinase pathway in hematopoietic stem cells and leukemia-initiating cells: a mechanistic difference between normal and cancer stem cells,* Blood Cells Mol. Dis., 41 (2008), pp. 73–76.